# Part I

# Physics Case

# Chapter 1

# The Physics Case for BTeV

## 1.1 Introduction

Experimental particle physics seeks answers to many questions about nature. Some central issues include:

- How are fermion masses generated?
- Why is there a family structure?
- Why are there three families rather than one?

The Standard Model [1] describes these phenomena quite well. Thus far all predictions are consistent with experiment. Symmetries and symmetry violations are crucially important physics phenomena. Weak decays are known to violate parity, P, and the product of charge-conjugation and parity, CP [2]. That the three family structure allows CP violation to occur naturally via quark mixing is an important clue that we are on the right track. However, the Standard Model is more of a description than an explanation.

The magnitude of CP violation is intimately tied to the question of "baryogenesis," or how did the Universe get rid of the anti-baryons. A possible solution was first proposed by Sakharov [3]. It requires three ingredients: CP violation, lack of thermal equilibrium at some time and baryon non-conservation. The Standard Model provides the third component via quantum corrections to anomaly diagrams. Inflation can provide the lack of thermal equilibrium. Although the Standard Model incorporates CP violation, it is believed that the amount is far too small. Of course we may find that the Standard Model explanation is incorrect.

We describe here a program of measurements that need to be performed in order to test whether the Standard Model indeed describes quark mixing and CP violation. There are many important experimental measurements to be made. We will describe the reasons why these measurements are crucial. We will also point out the important tests that probe for physics beyond the Standard Model.

There are many other interesting and important physics topics concerning issues of heavy quark production, the phenomenology of weak decays, etc., that we do not discuss here. It should be kept in mind that other areas of interesting physics can be addressed by BTeV.

## 1.2 The CKM Matrix

The physical point-like states of nature that have both strong and electroweak interactions, the quarks, are mixtures of base states described by the Cabibbo-Kobayashi-Maskawa (CKM) matrix [4],

$$\begin{pmatrix} d' \\ s' \\ b' \end{pmatrix} = \begin{pmatrix} V_{ud} & V_{us} & V_{ub} \\ V_{cd} & V_{cs} & V_{cb} \\ V_{td} & V_{ts} & V_{tb} \end{pmatrix} \begin{pmatrix} d \\ s \\ b \end{pmatrix} . \qquad (1.1)$$

The unprimed states are the mass eigenstates, while the primed states denote the weak eigenstates. The $V_{ij}$'s are complex numbers that can be represented by four independent real quantities. These numbers are fundamental constants of nature that need to be determined from experiment, like any other fundamental constant such as $\alpha$ or $G$. In the Wolfenstein approximation the matrix is written as [5]

$$V_{CKM} = \begin{pmatrix} 1-\lambda^2/2 & \lambda & A\lambda^3(\rho - i\eta(1-\lambda^2/2)) \\ -\lambda & 1-\lambda^2/2 - i\eta A^2\lambda^4 & A\lambda^2(1+i\eta\lambda^2) \\ A\lambda^3(1-\rho-i\eta) & -A\lambda^2 & 1 \end{pmatrix} . \qquad (1.2)$$

This expression is accurate to order $\lambda^3$ in the real part and $\lambda^5$ in the imaginary part. It is necessary to express the matrix to this order to have a complete formulation of the physics we wish to pursue. The constants $\lambda$ and $A$ have been measured using semileptonic $s$ and $b$ decays [6]; $\lambda \approx 0.22$ and $A \approx 0.8$. The phase $\eta$ allows for CP violation. There are experimental constraints on $\rho$ and $\eta$ that will be discussed below.

### 1.2.1 Unitarity Triangles

The unitarity of the CKM matrix[1] allows us to construct six relationships. These equations may be thought of as triangles in the complex plane. They are shown in Fig. 1.1

In the **bd** triangle, the one usually considered, the angles are all thought to be relatively large. It is described by:

$$V_{ub}V_{ud}^* + V_{cb}V_{cd}^* + V_{tb}V_{td}^* = 0 \quad . \qquad (1.3)$$

To a good approximation

$$|V_{ud}^*| \approx |V_{tb}| \approx 1, \qquad (1.4)$$

which implies

$$\frac{V_{ub}}{V_{cb}} + \frac{V_{td}^*}{V_{cb}} + V_{cd}^* = 0 \quad . \qquad (1.5)$$

[1]Unitarity implies that any pair of rows or columns are orthogonal.

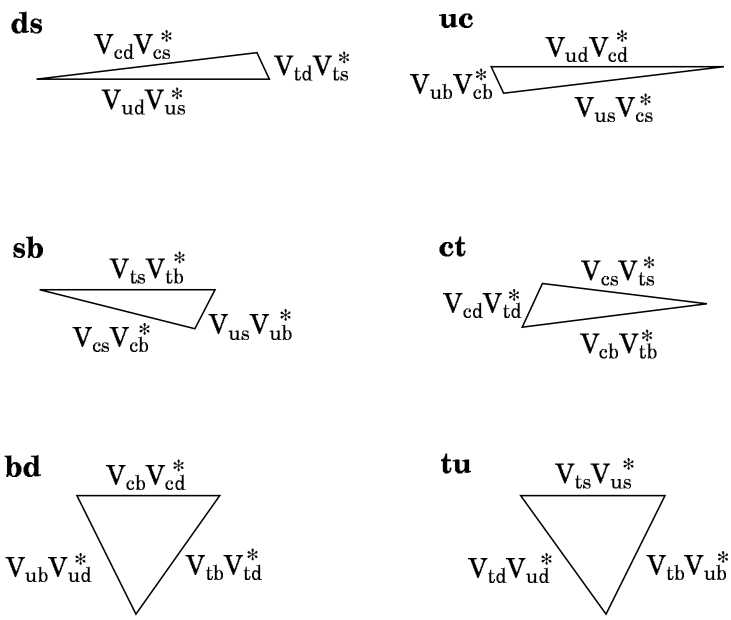


Figure 1.1: The six CKM triangles. The bold labels, i.e **ds** refer to the rows or columns used in the unitarity relationship.

Since $V_{cd}^* = \lambda$, we can define a triangle with sides

$$1 \tag{1.6}$$

$$\left|\frac{V_{td}}{A\lambda^3}\right| = \sqrt{(\rho-1)^2+\eta^2} = \frac{1}{\lambda}\left|\frac{V_{td}}{V_{ts}}\right| \tag{1.7}$$

$$\left|\frac{V_{ub}}{A\lambda^3}\right| = \sqrt{\rho^2+\eta^2} = \frac{1}{\lambda}\left|\frac{V_{ub}}{V_{cb}}\right| . \tag{1.8}$$

This CKM triangle is depicted in Fig. 1.2.

We know two sides already: the base is defined as unity and the left side is determined within a relatively large error by the measurements of $|V_{ub}/V_{cb}|$ [7]. The right side can be determined using mixing measurements in the neutral $B$ system. However, there is a very large error due to the uncertainty in $f_B$, the $B$-meson decay constant. Later we will discuss other measurements that can determine this side. The figure also shows the angles $\alpha$, $\beta$, and $\gamma$. These angles can be determined by measuring CP violation in the $B$ system.

Aleksan, Kayser and London [8] have shown that the CKM matrix can be expressed in terms of four independent phases. These are taken as:

$$\beta = arg\left(-\frac{V_{tb}V_{td}^*}{V_{cb}V_{cd}^*}\right), \qquad \gamma = arg\left(-\frac{V_{ub}^*V_{ud}}{V_{cb}^*V_{cd}}\right),$$

$$\chi = arg\left(-\frac{V_{cs}^*V_{cb}}{V_{ts}^*V_{tb}}\right), \qquad \chi' = arg\left(-\frac{V_{ud}^*V_{us}}{V_{cd}^*V_{cs}}\right), \tag{1.9}$$

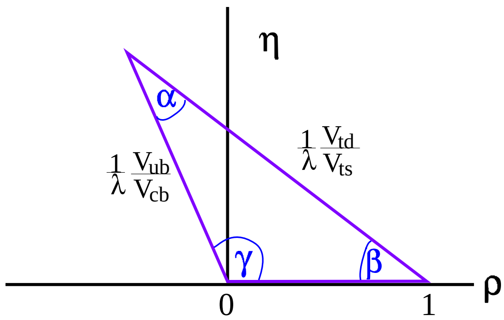


Figure 1.2: The CKM triangle shown in the $\rho - \eta$ plane. The left side is determined by $|V_{ub}/V_{cb}|$ and the right side can be determined using mixing in the neutral $B$ system. The angles can be found by making measurements of CP violation in $B$ decays.

where we have changed the confusing notation of Aleksan *et al* from $\epsilon$, $\epsilon'$ to $\chi$ and $\chi'$. We will address the usefulness of this parameterization in section 1.9.

### 1.2.2 Neutral $B$ Mixing

Neutral $B$ mesons can transform to their anti-particles before they decay. The diagrams for $B_d$ mixing are shown in Fig. 1.3. (The diagrams for $B_s$ mixing are similar with $s$ quarks replacing $d$ quarks.) Although $u$, $c$ and $t$ quark exchanges are all shown, the $t$ quark plays a dominant role, mainly due to its mass, since the amplitude of this process grows with the mass of the exchanged fermion.

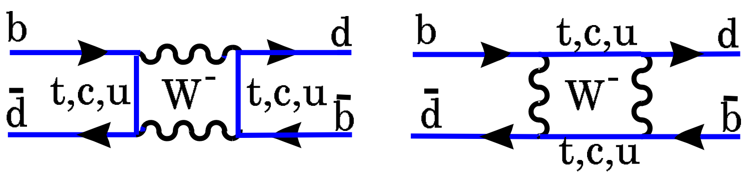


Figure 1.3: The two diagrams for $B_d$ mixing.

The probability of $B^o$ mixing is given by [9]

$$r = \frac{N\left(\overline{B}^o\right)}{N\left(B^o\right)} = \frac{x^2}{2+x^2}\ , \text{ where} \tag{1.10}$$

$$x \equiv \frac{\Delta m}{\Gamma} = \frac{G_F^2}{6\pi^2} B_B f_B^2 m_B \tau_B |V_{tb}^* V_{td}|^2 m_t^2 F\left(\frac{m_t^2}{M_W^2}\right) \eta_{QCD}, \tag{1.11}$$

where $B_B f_B^2$ is related to the probability of the $d$ and $\bar{b}$ quarks forming a hadron and must be estimated theoretically; $F$ is a known function which increases approximately as $m_t^2$, and $\eta_{QCD}$ is a QCD correction, with a value $\approx 0.8$ [10]. By far the largest uncertainty arises from the unknown decay constant, $f_B$. This number gives the coupling between the $B$ and the $W^-$. It could in principle be determined by finding the decay rate of $B^+ \to \mu^+\nu$ or $B^+ \to \tau^+\nu$, both of which are very difficult to measure. Since

$$|V_{tb}^* V_{td}|^2 \propto |(1-\rho-i\eta)|^2 = (\rho-1)^2 + \eta^2, \tag{1.12}$$

measuring mixing gives a circle centered at (1,0) in the $\rho-\eta$ plane. The best recent mixing measurements have come from a variety of sources [11], yielding a value (for $B_d$) of $\Delta m = (0.464 \pm 0.018) \times 10^{12}\,\hbar s^{-1}$.

The right-hand side of the triangle can be determined by measuring $B_s$ mixing using the ratio

$$\frac{\Delta m_s}{\Delta m_d} = \left(\frac{B_s}{B}\right)\left(\frac{f_{B_s}}{f_B}\right)^2\left(\frac{m_{B_s}}{m_B}\right)\left|\frac{V_{ts}}{V_{td}}\right|^2, \tag{1.13}$$

where

$$\left|\frac{V_{td}}{V_{ts}}\right|^2 = \lambda^2\left[(\rho-1)^2+\eta^2\right]. \tag{1.14}$$

The large uncertainty in using the $B_d$ mixing measurement to constrain $\rho$ and $\eta$ is largely removed since many sources of theoretical uncertainty cancel in the ratio of the first two factors in equation (1.13), which is believed to be known to $\pm 20\%$ [12].

### 1.2.3 Current Status of the CKM Matrix

Measurements of $|V_{ub}/V_{cb}|$ probe $\rho^2+\eta^2$ and thus form a circular constraint in the $\rho-\eta$ plane centered at (0,0). Similarly, mixing measurements form a circular constraint centered on (1,0).

The fact that the CKM matrix is complex allows CP violation. There is a constraint on $\rho$ and $\eta$ given by the $K_L^o$ CP violation measurement ($\epsilon$), given by [13]

$$\eta\left[(1-\rho)A^2(1.4\pm0.2)+0.35\right]A^2\frac{B_K}{0.75} = (0.30\pm0.06), \tag{1.15}$$

where the errors arise from uncertainties on $m_t$ and $m_c$.

The constraints on $\rho$ versus $\eta$ from the $V_{ub}/V_{cb}$ measurement, $\epsilon$ and $B$ mixing are shown in Fig. 1.4. The bands represent $1\sigma$ errors, for the measurements, and a 95% confidence level upper limit on $B_s$ mixing. The width of the $B_d$ mixing band is caused mainly by the uncertainty on $f_B$, taken here as $240 > f_B > 160$ MeV. Other parameters include $|V_{cb}| = 0.0381 \pm 0.0021$, $|V_{ub}/V_{cb}| = 0.085 \pm 0.019$ [14], limit on $\Delta m_s > 12.4$ ps$^{-1}$, and the ratio $f_{B_s}\sqrt{B_{B_s}}/f_{B_d}\sqrt{B_{B_d}} \leq 1.25$ [15].

The width of the $\epsilon$ band is caused by errors in $A$, $m_t$, $m_c$ and $B_K$. Here $B_K$ is taken as 0.80$\pm$0.15 according to Buras [16].

Recent measurements of $\epsilon'/\epsilon$ determine $\eta$ directly [2]. However, the theoretical errors are so large that all that can be said is that the measurement is consistent with the allowed region. We caution the reader that this plot is only a guide, since the measured quantities

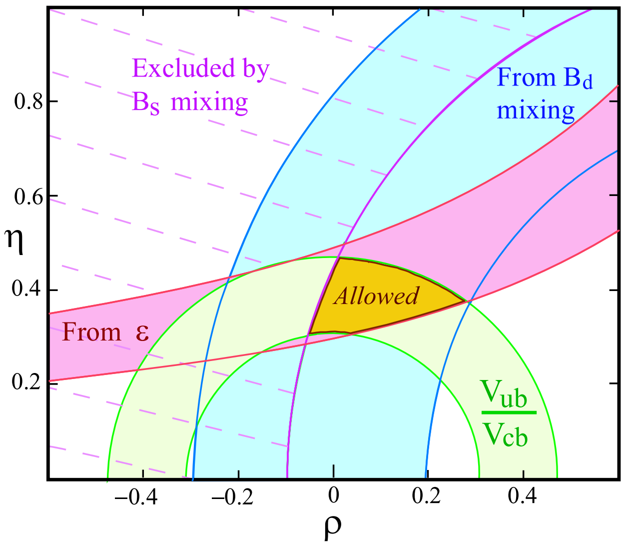


Figure 1.4: The regions in $\rho-\eta$ space (shaded) consistent with measurements of CP violation in $K_L^o$ decay ($\epsilon$), $V_{ub}/V_{cb}$ in semileptonic $B$ decay, $B_d^o$ mixing, and the excluded region from limits on $B_s^o$ mixing. The allowed region is defined by the overlap of the 3 permitted areas, and is where the apex of the CKM triangle sits.

all have large or even dominant errors due to theoretical models, and the bands are only $\pm 1\sigma$ wide. This analysis is in good agreement with that of Rosner [15]. and in substantial agreement with the analysis of Plaszczynski and Schune [17], but not in agreement with Caravaglios *et al* [18], who extract what we view as unreasonably small errors from the data.

## 1.3 CP Violation in Charged $B$ Decays

The theoretical basis of the study of CP violation in $B$ decays was given in a series of papers by Carter and Sanda, and Bigi and Sanda [19]. We start with charged $B$ decays. Consider the final states $f^{\pm}$ which can be reached by two distinct weak processes with amplitudes $\mathcal{A}$ and $\mathcal{B}$, respectively.

$$\mathcal{A} = a_s e^{i\theta_s} a_w e^{i\theta_w}, \quad \mathcal{B} = b_s e^{i\delta_s} b_w e^{i\delta_w} \quad . \tag{1.16}$$

The strong phases are denoted by the subscript $s$ and weak phases are denoted by the subscript $w$. Under the CP operation the strong phases are invariant but the weak phases change sign, so

$$\overline{\mathcal{A}} = a_s e^{i\theta_s} a_w e^{-i\theta_w}, \quad \overline{\mathcal{B}} = b_s e^{i\delta_s} b_w e^{-i\delta_w} \quad . \tag{1.17}$$

The rate difference is

$$\Gamma - \overline{\Gamma} = |\mathcal{A} + \mathcal{B}|^2 - |\overline{\mathcal{A}} + \overline{\mathcal{B}}|^2 \tag{1.18}$$

$$= 2 a_s a_w b_s b_w \sin(\delta_s - \theta_s) \sin(\delta_w - \theta_w) \quad . \tag{1.19}$$

A weak phase difference is guaranteed in the appropriate decay mode (different CKM phases), but the strong phase difference is not; it is very difficult to predict the magnitude of strong phase differences.

As an example consider the possibility of observing CP violation by measuring a rate difference between $B^- \to K^-\pi^o$ and $B^+ \to K^+\pi^o$. The $K^-\pi^o$ final state can be reached either by tree or penguin diagrams as shown in Fig. 1.5. The tree diagram has an imaginary

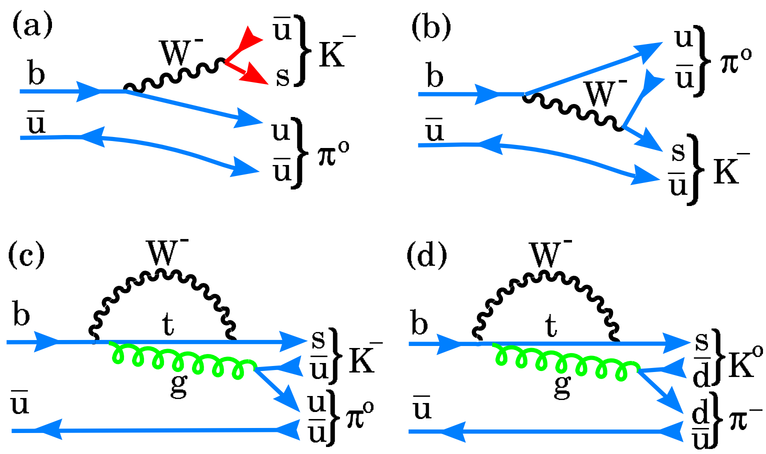


Figure 1.5: Diagrams for $B^- \to K^-\pi^o$, (a) and (b) are tree level diagrams where (b) is color suppressed; (c) is a penguin diagram. (d) shows $B^- \to K^o\pi^-$, which cannot be produced via a tree diagram.

part coming from the $V_{ub}$ coupling, while the penguin term does not, thus insuring a weak phase difference. This type of CP violation is called "direct." Note also that the process $B^- \to K^o\pi^-$ can only be produced by the penguin diagram in Fig. 1.5(d). Therefore, in this simple example, we do not expect a rate difference between $B^- \to K^o\pi^-$ and $B^+ \to K^o\pi^+$. (There have been suggestions that rescattering effects may contribute here and produce a rate asymmetry, see section 1.8.)

## 1.4 CP Violation Formalism in Neutral $B$ decays

For neutral mesons we can construct the CP eigenstates

$$|B_1^o\rangle = \frac{1}{\sqrt{2}}\left(|B^o\rangle + |\overline{B}^o\rangle\right) \quad , \tag{1.20}$$

$$|B_2^o\rangle = \frac{1}{\sqrt{2}}\left(|B^o\rangle - |\overline{B}^o\rangle\right) \quad , \tag{1.21}$$

where

$$CP|B_1^o\rangle = |B_1^o\rangle \quad , \tag{1.22}$$

$$CP|B_2^o\rangle = -|B_2^o\rangle \quad . \tag{1.23}$$

Since $B^o$ and $\overline{B}^o$ can mix, the mass eigenstates are superpositions of $a|B^o\rangle + b|\overline{B}^o\rangle$ which obey the Schrödinger equation

$$i\frac{d}{dt}\begin{pmatrix} a \\ b \end{pmatrix} = H\begin{pmatrix} a \\ b \end{pmatrix} = \left(M - \frac{i}{2}\Gamma\right)\begin{pmatrix} a \\ b \end{pmatrix}. \tag{1.24}$$

If CP is not conserved then the eigenvectors, the mass eigenstates $|B_L\rangle$ and $|B_H\rangle$, are not the CP eigenstates but are

$$|B_L\rangle = p|B^o\rangle + q|\overline{B}^o\rangle, \quad |B_H\rangle = p|B^o\rangle - q|\overline{B}^o\rangle, \tag{1.25}$$

where

$$p = \frac{1}{\sqrt{2}}\frac{1+\epsilon_B}{\sqrt{1+|\epsilon_B|^2}}, \quad q = \frac{1}{\sqrt{2}}\frac{1-\epsilon_B}{\sqrt{1+|\epsilon_B|^2}}. \tag{1.26}$$

CP is violated if $\epsilon_B \neq 0$, which occurs if $|q/p| \neq 1$.

The time dependence of the mass eigenstates is

$$\begin{aligned} |B_L(t)\rangle &= e^{-\Gamma_L t/2} e^{-im_L t/2}|B_L(0)\rangle & (1.27)\\ |B_H(t)\rangle &= e^{-\Gamma_H t/2} e^{-im_H t/2}|B_H(0)\rangle, & (1.28) \end{aligned}$$

leading to the time evolution of the flavor eigenstates as

$$|B^o(t)\rangle = e^{-\left(im+\frac{\Gamma}{2}\right)t}\left(\cos\frac{\Delta m t}{2}|B^o(0)\rangle + i\frac{q}{p}\sin\frac{\Delta m t}{2}|\overline{B}^o(0)\rangle\right) \tag{1.29}$$

$$|\overline{B}^o(t)\rangle = e^{-\left(im+\frac{\Gamma}{2}\right)t}\left(i\frac{p}{q}\sin\frac{\Delta m t}{2}|B^o(0)\rangle + \cos\frac{\Delta m t}{2}|\overline{B}^o(0)\rangle\right), \tag{1.30}$$

where $m = (m_L + m_H)/2$, $\Delta m = m_H - m_L$ and $\Gamma = \Gamma_L \approx \Gamma_H$. Note that the fraction of $B^o$ remaining at time $t$ is given by $\langle B^o(t)|B^o(t)\rangle^*$, and is a pure exponential, $e^{-\Gamma t}$, in the absence of CP violation.

*Indirect CP violation in the neutral B system*

As in the case of $K_L$ decay, we can look for the rate asymmetry

$$\begin{aligned} a_{sl} &= \frac{\Gamma\left(\overline{B}^o(t) \to X\ell^+\nu\right) - \Gamma\left(B^o(t) \to X\ell^-\overline{\nu}\right)}{\Gamma\left(\overline{B}^o(t) \to X\ell^+\nu\right) + \Gamma\left(B^o(t) \to X\ell^-\overline{\nu}\right)} & (1.31)\\ &= \frac{1 - \left|\frac{q}{p}\right|^4}{1 + \left|\frac{q}{p}\right|^4} \approx O\left(10^{-3}\right). & (1.32) \end{aligned}$$

These final states occur only through mixing as the direct decay occurs only as $B^o \to X\ell^+\nu$. To generate CP violation we need an interference between two diagrams. In this case the two diagrams are the mixing diagram with the $t$-quark and the mixing diagram with the $c$-quark. This is identical to what happens in the $K_L^o$ case. This type of CP violation is called "indirect." The small size of the expected asymmetry is caused by the off-diagonal elements of the $\Gamma$ matrix in equation (1.24) being very small compared to the off-diagonal elements of the mass matrix, i.e. $|\Gamma_{12}/M_{12}| \ll 1$ and $\mathrm{Im}(\Gamma_{12}/M_{12}) \neq 0$. This results from the nearly equal widths of the $B_L^o$ and $B_H^o$ [20].

In the case of the $B_s^o$ a relatively large, $\approx$15% component of $B_s$ decays is predicted to end up as a $c\bar{c}s\bar{s}$ final state. Since $\overline{B}_s$ decays with the same rate into the same final state, it has been predicted [21] [23] [22] that there will be a substantial width difference $\Delta\Gamma = \Gamma_H - \Gamma_L \approx 15\%\Gamma$, between CP+ and CP- eigenstates. BTeV can easily measure this lifetime difference by measuring the lifetime of a mixed CP state such as $D_s^+\pi^-$ and comparing with the CP- state $J/\psi\eta'$. The CP+ state $K^+K^-$ can also be used [24]. For finite $\Delta\Gamma$, equations 1.29 and 1.30 are modified [25]. See section 1.8.5 for more details.

*CP violation for $B$ via interference of mixing and decays*

Here we choose a final state $f$ which is accessible to both $B^o$ and $\overline{B}^o$ decays. The second amplitude necessary for interference is provided by mixing. Fig. 1.6 shows the decay into $f$ either directly or indirectly via mixing. It is necessary only that $f$ be accessible from either

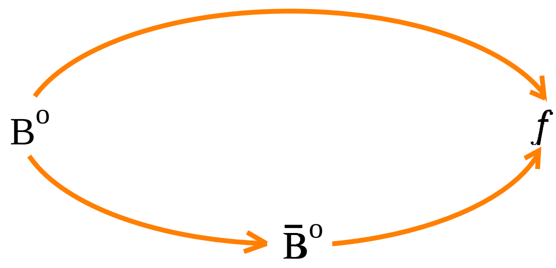


Figure 1.6: Two interfering ways for a $B^o$ to decay into a final state $f$.

state. However if $f$ is a CP eigenstate the situation is far simpler. For CP eigenstates

$$CP|f_{CP}\rangle = \pm|f_{CP}\rangle. \tag{1.33}$$

It is useful to define the amplitudes

$$A = \langle f_{CP}|\mathcal{H}|B^o\rangle, \quad \bar{A} = \langle f_{CP}|\mathcal{H}|\overline{B}^o\rangle. \tag{1.34}$$

If $\left|\frac{\bar{A}}{A}\right| \neq 1$, then we have "direct" CP violation in the decay amplitude, which was discussed above. Here CP can be violated by having

$$\lambda = \frac{q}{p}\cdot\frac{\bar{A}}{A} \neq 1, \tag{1.35}$$

which requires only that $\lambda^2$ acquire a non-zero phase, i.e. $|\lambda|$ could be unity and CP violation can occur.

The asymmetry, in this case, is defined as

$$a_{f_{CP}} = \frac{\Gamma\left(B^o(t) \to f_{CP}\right) - \Gamma\left(\overline{B}^o(t) \to f_{CP}\right)}{\Gamma\left(B^o(t) \to f_{CP}\right) + \Gamma\left(\overline{B}^o(t) \to f_{CP}\right)}, \tag{1.36}$$

which for $|q/p| = 1$ gives

$$a_{f_{CP}} = \frac{\left(1 - |\lambda|^2\right)\cos\left(\Delta m t\right) - 2\mathrm{Im}\lambda\sin(\Delta m t)}{1 + |\lambda|^2}. \tag{1.37}$$

For the cases where there is only one decay amplitude $A$, $|\lambda|$ equals 1, and we have

$$a_{f_{CP}} = -\mathrm{Im}\lambda\sin(\Delta m t). \tag{1.38}$$

Only the amplitude, $-\mathrm{Im}\lambda$ contains information about the level of CP violation, the sine term is determined only by $B^o$ mixing. In fact, the time integrated asymmetry is given by

$$a_{f_{CP}} = -\frac{x}{1+x^2}\mathrm{Im}\lambda \ , \tag{1.39}$$

where $x = \frac{\Delta m}{\Gamma}$. For the case of the $B_d^o$, $x/(1+x^2)$= 0.48, which is quite lucky as the maximum size of the coefficient is $-0.5$.

$\mathrm{Im}\lambda$ is related to the CKM parameters. Recall $\lambda = \frac{q}{p} \cdot \frac{\bar{A}}{A}$. The first term is the part that comes from mixing:

$$\frac{q}{p} = \frac{\left(V_{tb}^* V_{td}\right)^2}{\left|V_{tb}V_{td}\right|^2} = \frac{\left(1-\rho-i\eta\right)^2}{\left(1-\rho+i\eta\right)\left(1-\rho-i\eta\right)} = e^{-2i\beta} \quad \text{and} \tag{1.40}$$

$$\mathrm{Im}\frac{q}{p} = -\frac{2(1-\rho)\eta}{\left(1-\rho\right)^2+\eta^2} = \sin(2\beta). \tag{1.41}$$

To evaluate the decay part we need to consider specific final states. For example, consider $f \equiv \pi^+\pi^-$. The simple spectator decay diagram is shown in Fig. 1.7. For the moment we will assume that this is the only diagram which contributes. Later we will show why this is not true. For this $b \to u\bar{u}d$ process we have

$$\frac{\bar{A}}{A} = \frac{\left(V_{ud}^* V_{ub}\right)^2}{\left|V_{ud}V_{ub}\right|^2} = \frac{(\rho-i\eta)^2}{(\rho-i\eta)(\rho+i\eta)} = e^{-2i\gamma}, \tag{1.42}$$

and

$$\mathrm{Im}(\lambda) = \mathrm{Im}(e^{-2i\beta}e^{-2i\gamma}) = \mathrm{Im}(e^{2i\alpha}) = \sin(2\alpha) \ . \tag{1.43}$$

[2] $\lambda$ here is not the same variable that occurs in the Wolfenstein representation of the CKM matrix.

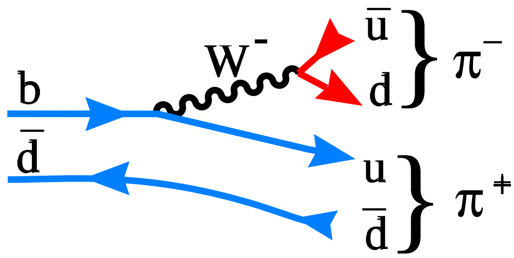


Figure 1.7: Decay diagram at the tree level for $B^o \to \pi^+\pi^-$.

The final state $J/\psi K_S$ plays an especially important role in the study of CP violation. It is a CP eigenstate and its decay is dominated by only one diagram, shown in Fig. 1.8. In this case we do not get a phase from the decay part because

$$\frac{\bar{A}}{A} = \frac{(V_{cb}V_{cs}^*)^2}{|V_{cb}V_{cs}|^2} \tag{1.44}$$

is real. In this case the final state is a state of negative $CP$, i.e. $CP|J/\psi K_S\rangle = -|J/\psi K_S\rangle$.

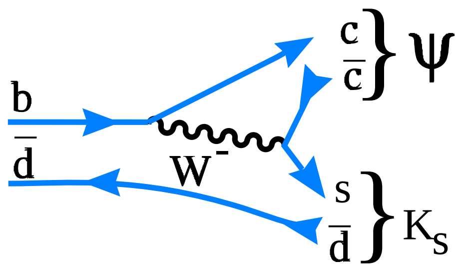


Figure 1.8: Decay diagram at the tree level for $B^o \to J/\psi K_S$.

This introduces an additional minus sign in the result for Im$\lambda$. Before finishing discussion of this final state we need to consider in more detail the presence of the $K_S$ in the final state. Since neutral kaons can mix, we pick up another mixing phase. This term creates a phase given by

$$\left(\frac{q}{p}\right)_K = \frac{(V_{cd}^* V_{cs})^2}{|V_{cd}V_{cs}|^2}, \tag{1.45}$$

which is zero. It is necessary to include this term, however, since there are other formulations of the CKM matrix than Wolfenstein, which have the phase in a different location. It is important that the physics predictions not depend on the CKM convention.[3]

In summary, for the case of $f = J/\psi K_S$, Im$\lambda = -\sin(2\beta)$.

[3]Here we don't include CP violation in the neutral kaon since it is much smaller than what is expected in the $B$ decay.

## 1.5 Techniques for Determining $\beta$

The decay $B^o \to J/\psi K_S$ is the primary source for measurements of $\sin(2\beta)$. In the common phase convention, CP violation is expected to arise mostly from the mixing, driven by $\mathrm{Im}(q/p)$, while the decay amplitude, $\mathrm{Im}(\bar{A}/A)$, is expected to contribute only a small part (see Fig. 1.8). This decay is expected to have only a small Penguin contribution, but even if the Penguin contribution is significant it does not change the contribution of the mixing phase or the decay phase.[4]

While we expect that $\sin(2\beta)$ will have been measured before BTeV, we do aim to improve significantly on the precision of the measurement. Furthermore, we intend to be able to remove "ambiguities." When we measure $\sin(2\phi)$, where $\phi$ is any angle, we have a four-fold ambiguity in $\phi$, namely $\phi$, $\pi/2-\phi$, $\phi+\pi$ and $3\pi/2-\phi$. These ambiguities can mask the effects of new physics. Our task is to remove as many of the ambiguities as possible.

### 1.5.1 Removal of Two of the $\beta$ Ambiguities

The decay $B \to J/\psi\, K^*(890)$, where $K^* \to K_S\pi^o$ can be used to get information about the sign of $\cos(2\beta)$, which would remove two of the ambiguities [26]. This decay is described by three complex decay amplitudes. Following a suggestion of Dighe, Dunietz, and Fleischer [27, 28], we write the decay amplitudes $A_0 = -\sqrt{1/3}\,S + \sqrt{2/3}\,D$, $A_{||} = \sqrt{2/3}\,S + \sqrt{1/3}\,D$, and $A_\perp = P$, where $S$, $P$, and $D$ denote S, P, and D wave amplitudes, respectively. Normalizing the decay amplitudes to $|A_0|^2 + |A_{||}|^2 + |A_\perp|^2 = 1$ and eliminating one overall phase leaves four independent parameters.

The full angular distribution of a $B$ meson decaying into two vector particles is specified by three angles. The helicity angle basis [29] has been used for angular analyses of $B \to J/\psi\, K^*$ decays. An alternative basis, called the transversity basis is more suitable for extracting parity information [28].

In the transversity basis, the direction of the $K^*$ in the $J/\psi$ rest frame defines the x-axis of a right-handed coordinate system. The $K\pi$ plane fixes the y-axis with $p_y(K) > 0$ and the normal to this plane defines the z-axis. The transversity angles $\theta_{\rm tr}$ and $\phi_{\rm tr}$ are then defined as polar and azimuth angles of the $l^+$ in the $J/\psi$ rest frame. The third angle, the $K^*$ decay angle $\theta_{K^*}$, is defined as that of the $K$ in the $K^*$ rest frame relative to the negative of the $J/\psi$ direction in that frame. Using these definitions the full angular distribution of the $B \to J/\psi\, K^*$ decay is [28]:

$$
\begin{aligned}
&\frac{1}{\Gamma}\,\frac{\mathrm{d}^3\Gamma}{\mathrm{d}\cos\theta_{\rm tr}\,\mathrm{d}\cos\theta_{K^*}\,\mathrm{d}\phi_{\rm tr}} \\
&\quad = \tfrac{9}{32\pi}\,\{2\,|A_0|^2\,\cos^2\theta_{K^*}(1-\sin^2\theta_{\rm tr}\cos^2\phi_{\rm tr}) \\
&\qquad\quad + |A_{||}|^2\,\sin^2\theta_{K^*}(1-\sin^2\theta_{\rm tr}\sin^2\phi_{\rm tr}) \\
&\qquad\quad + |A_\perp|^2\,\sin^2\theta_{K^*}\sin^2\theta_{\rm tr}\sin^2\phi_{\rm tr}
\end{aligned}
$$

[4]Actually the only phase that has physical meaning is the product of $q/p \cdot \bar{A}/A$.

$$
\begin{aligned}
&- \operatorname{Im}(A_{\|}^{*}A_{\perp})\ \sin^2\theta_{K^*}\sin 2\theta_{\rm tr}\sin\phi_{\rm tr} \\
&+ \tfrac{1}{\sqrt{2}}\operatorname{Re}(A_0^{*}A_{\|})\ \sin 2\theta_{K^*}\sin^2\theta_{\rm tr}\sin 2\phi_{\rm tr} \\
&+ \tfrac{1}{\sqrt{2}}\operatorname{Im}(A_0^{*}A_{\perp})\ \sin 2\theta_{K^*}\sin 2\theta_{\rm tr}\cos\phi_{\rm tr}\ \}.
\end{aligned}
\tag{1.46}
$$

For $\bar{B}$ decays the interference terms containing $A_\perp$ switch sign while all other terms remain unchanged.

Results shown in Table 1.1 have been obtained from CLEO and CDF using the decay $\bar{K}^{*o} \to K^-\pi^+$.

| Parameter | CLEO [30] | CDF [31] |
|---|---|---|
| $\lvert A_0\rvert^2 = \Gamma_{\rm L}/\Gamma$ | $0.52 \pm 0.07 \pm 0.04$ | $0.59 \pm 0.06 \pm 0.02$ |
| $\lvert A_\perp\rvert^2 = \lvert P\rvert^2$ | $0.16 \pm 0.08 \pm 0.04$ | $0.13\,^{+0.12}_{-0.06} \pm 0.03$ |

Table 1.1: Resulting decay amplitudes from the fit to the transversity angles. The first error is statistical and the second is the estimated systematic uncertainty.

The parity odd component, $|A_\perp|^2$, is three standard deviations from zero in the average of the two experiments, and is $\approx$25% of the rate of the parity even component. This is likely large enough to allow the determination of the sign of the interference terms using the tagged $K^{*o} \to K_S\pi^o$ decays; that, in turn, allows a determination of the sign of the product of $\cos(2\beta)$ with a strong phase-shift. The sign of this phase-shift can either be obtained from factorization, which is a dangerous procedure, or using the much weaker assumption of SU(3) symmetry, and analyzing the time-dependent oscillations in the decay $B_s \to J/\psi\phi$ [26], where the mixing phase is expected to be small.

Another independent method of removing two of the ambiguities is to measure the sign of the $\cos(2\beta)$ term in the decay $B^o \to J/\psi K^o$, $K^o \to \pi^\pm\ell^\mp\nu$. This idea developed by Kayser [32], works because of the interference between $K_L$ and $K_S$ in the decay, where the decay amplitudes are equal. The time evolution of the decay width can be expressed in terms of the $B^o$ decay time ($t_B$) and the $K^o$ decay time ($t_K$) as

$$
\begin{aligned}
\Gamma(t_B, t_K) \propto\ & \\
& e^{-\Gamma_B t_B}\Big\{ e^{-\gamma_s t_K}\left[1 \mp sin(2\beta) sin(\Delta m_B t_B)\right] \\
&\qquad + e^{-\gamma_L t_K}\left[1 \pm sin(2\beta) sin(\Delta m_B t_B)\ \right] \\
&\qquad \pm(\mp) 2 e^{-\frac{1}{2}(\gamma_s+\gamma_L)t_K}\big[\ \cos(\Delta m_B t_B)\cos(\Delta m_K t_K) \\
&\qquad\qquad + \cos(2\beta) sin(\Delta m_B t_B) sin(\Delta m_K t_K)\big]\ \Big\},
\end{aligned}
\tag{1.47}
$$

where the top sign of each pair is for $B^o$, and the bottom for $\overline{B}^o$. The first pair of signs in the third line refers to the kaon decay mode $\pi^-\ell^+\nu$ ($K$), while the second pair is for $\pi^+\ell^-\bar{\nu}$ ($\overline{K}$).

To get an idea of the predicted asymmetries, we integrate this equation over $t_B$. There are four different rates that can be denoted as combinations of $B$ and $\overline{B}$ with $K$ and $\overline{K}$. In Fig. 1.9 we show the four rates as solid lines if $\cos(2\beta)$ were positive and the four rates as dashed lines if $\cos(2\beta)$ were negative. These were done for $\sin(2\beta) = 0.7$. If $\sin(2\beta)$ were smaller the rate differences would be larger and vice-versa.

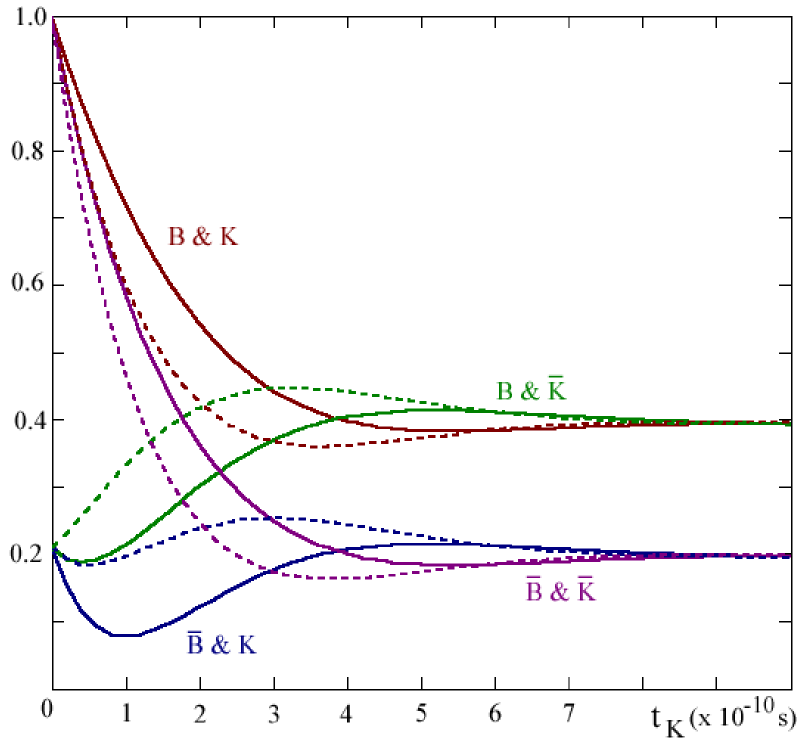


Figure 1.9: The decay rates for $B^o \to J/\psi K^o$, $K^o \to \pi\ell\nu$, as a function of $K^o$ decay time, integrated over the $B^o$ decay time. The solid lines have the sign of the $\cos(2\beta)$ term as positive, while the corresponding dashed lines have negative values. The absolute normalization is arbitrary, and $\sin(2\beta)$ was fixed at 0.7.

The differences are large over about five $K_S$ lifetimes. Since only the sign of the $\cos(2\beta)$ term needs to be found, all other parameters, including $\sin(2\beta)$ are specified. Unfortunately, the event rate is rather small, since $\mathcal{B}(K_S \to \pi\ell\nu) = 1.4 \times 10^{-3}$ and although $\mathcal{B}(K_L \to \pi\ell\nu) = 0.66$, only 1% of the $K_L$ decay soon enough to be of use. Roughly, we have about 100 times fewer events than in $J/\psi K_S$. However, if the backgrounds are not too large, it will only take on the order of a hundred events to successfully determine the sign of $\cos(2\beta)$ using this technique.

It is interesting to note that measuring this combination of $B^o$ and $K^o$ decay modes can lead to measurements of CPT violation [33].

## 1.6 Comment on Penguin Amplitude

Many processes can have penguin components. The diagram for $B^o \to \pi^+\pi^-$ is shown in Fig. 1.10. The $\pi^+\pi^-$ final state is expected to have a rather large penguin amplitude ~20% of the tree amplitude. Then $|\lambda| \neq 1$ and $a_{f_{CP}}$, equation 1.37, develops a $\cos(\Delta m t)$ term. In the $J/\psi K_S$ case, the penguin amplitude is expected to be small since a $c\bar{c}$ pair must be

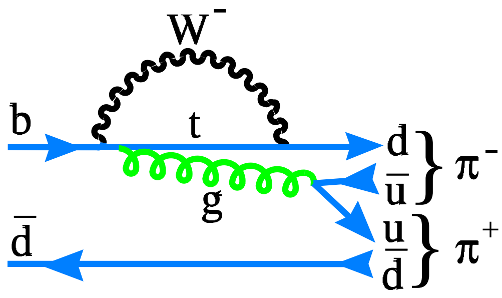


Figure 1.10: Penguin diagram for $B^o \to \pi^+\pi^-$.

"popped" from the vacuum. Even if the penguin decay amplitude were of significant size, the decay phase, $\text{Im}(\overline{A}/A)$ is the same as the tree level process, and quite small.

## 1.7 Techniques for Determining $\alpha$

Measuring $\alpha$ is more difficult than measuring $\beta$ in several respects. First of all, the decay amplitudes are modulated by $V_{ub}$ rather than $V_{cb}$, making the overall rates small. Secondly, the gluonic Penguin rates are of the same order causing well known difficulties in extracting the weak phase angle (see section 1.6 above). The Penguin diagrams add a third amplitude to the tree level and mixing amplitudes. It turns out, however, that this complication can be a blessing in disguise. The interference generates $\cos(2\alpha)$ terms in the decay rate, that can be used to remove discrete ambiguities.

The decay $B^o \to \pi^+\pi^-$ has oft been cited as a way to measure $\sin(2\alpha)$. However, the Penguin pollution mentioned above, makes it difficult to extract the angle. Current data from CLEO gives $\mathcal{B}(B^o \to K^\mp\pi^\pm) = (1.72^{+0.25}_{-0.24} \pm 0.12) \times 10^{-5}$ and $\mathcal{B}(B^o \to \pi^+\pi^-) = (0.43^{+0.16}_{-0.14} \pm 0.05) \times 10^{-5}$ [34], showing a relatively large Penguin amplitude which cannot be ignored. Gronau and London [35] have shown that an isospin analysis using the additional decays $B^- \to \pi^-\pi^o$ and $B^o \to \pi^o\pi^o$ can be used to extract $\alpha$ [36], but the $\pi^o\pi^o$ final state is extremely difficult to detect in any existing or proposed experiment. Other authors have suggested different methods [37], but they all have theoretical assumptions. Thus, measurement of the CP asymmetry in $B^o \to \pi^+\pi^-$ cannot, in our view, provide an accurate determination of $\sin(2\alpha)$ unless some new breakthrough in theory occurs.

There is however, a theoretically clean method to determine $\alpha$. The interference between Tree and Penguin diagrams can be exploited by measuring the time dependent CP violating effects in the decays $B^o \to \rho\pi$ as shown by Snyder and Quinn [38]. There are three such neutral decay modes, listed in Table 1.2 with their respective Penguin and Tree amplitudes, denoted by $T^{ij}$, where $i$ lists charge of the $\rho$ and $j$ the charge of the $\pi$. For the $\rho^o\pi^o$ mode, isospin constraints are used to eliminate $T^{oo}$. The amplitudes for the charged decays are also given.

Table 1.2: $B^o \to \rho\pi$ Decay Modes

| Decay Mode | Decay Amplitudes |
|---|---|
| $\sqrt{2}A(B^+ \to \rho^+\pi^o)$ | $=S_1 = T^{+o} + 2P_1$ |
| $\sqrt{2}A(B^+ \to \rho^o\pi^+)$ | $=S_2 = T^{o+} - 2P_1$ |
| $A(B^o \to \rho^+\pi^-)$ | $=S_3 = T^{+-} + P_1 + P_o$ |
| $A(B^o \to \rho^-\pi^+)$ | $=S_4 = T^{-+} - P_1 + P_o$ |
| $2A(B^o \to \rho^o\pi^o)$ | $=S_5 = T^{+-} + T^{+-} - T^{+o} - T^{o+} - 2P_o$ |

For the $\rho\pi$ final state, the $\rho$ decay amplitude can be parameterized as

$$f(m,\theta) = \frac{\cos(\theta)\Gamma_\rho}{2(m_\rho - m - i0.5\Gamma_\rho)} \quad , \tag{1.48}$$

where $m_\rho$ is the $\rho$ mass of 0.77 GeV and $\Gamma_\rho$, the width of 0.15 GeV. $\theta$ is the helicity decay angle and the $\cos(\theta)$ dependence arises because the $\rho$ must be fully polarized in this decay which starts with a spin-0 $B$ and ends with a spin-1 $\rho$ and spin-0 $\pi$.

The full decay amplitudes for $B^o \to \rho\pi \to \pi^+\pi^-\pi^o$ and the corresponding $\overline{B}^o$ decay are given by

$$\begin{aligned} A(B^o) &= f^+S_3 + f^-S_4 + f^oS_5/2 \\ A(\overline{B}^o) &= f^+\overline{S}_3 + f^-\overline{S}_4 + f^o\overline{S}_5/2 \quad , \end{aligned} \tag{1.49}$$

where the superscript on the $f$ indicates the charge of the $\rho$. The sum over the three neutral $B$ decay amplitudes involves only tree amplitudes; the Penguins vanish. The angle between this sum for $B^o$ decays ($\equiv T$) and the sum for $\overline{B}^o$ ($\equiv \overline{T}$) is precisely $\alpha$. Computing the amplitudes gives a series of terms which have both $\sin(\Delta mt)$ and $\cos(\Delta mt)$ time dependences and coefficients which depend on both $\sin(2\alpha)$ and $\cos(2\alpha)$.

To extract $\alpha$ only the neutral modes need be measured. Further constraints and information about Penguin phases can be extracted if the charged $B$'s are also measured. But this is difficult because there are two $\pi^o$'s in the $\rho^+\pi^o$ decay mode.

The $\rho\pi$ final state has many advantages. First of all, it has a relatively large branching ratio. The latest CLEO measurement for the $\rho^o\pi^+$ final state is $(1.0 \pm 0.3 \pm 0.2) \times 10^{-5}$ [34]. The rate for the neutral $B$ final state $\rho^\pm\pi^\mp$ is $(2.8^{+0.8}_{-0.7} \pm 0.4) \times 10^{-5}$, while the $\rho^o\pi^o$ final state is limited at 90% confidence level to $< 5.1 \times 10^{-6}$ [39]. These measurements are consistent with theoretical expectations [40]. Secondly, since the $\rho$ is fully polarized in the

(1,0) configuration, it decays as $\cos^2\theta$, where $\theta$ is the angle of one of the $\rho$ decay products with the $\pi$ in the $\rho$ rest frame. This causes the periphery of the Dalitz plot to be heavily populated, especially the corners. A sample Dalitz plot is shown in Fig. 1.11. This kind of distribution is good for maximizing the interferences, which helps minimize the error. Furthermore, little information is lost by excluding the Dalitz plot interior, a good way to reduce backgrounds.

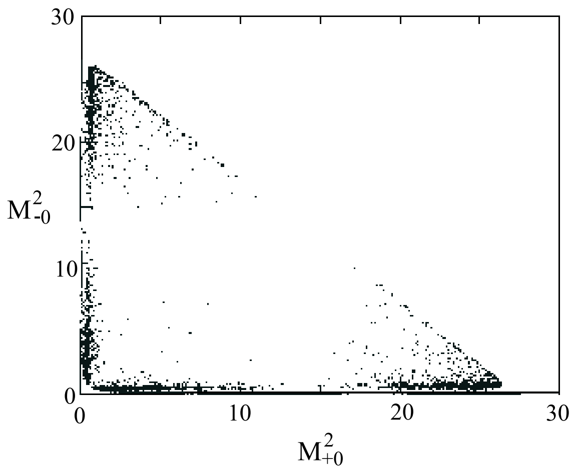


Figure 1.11: The Dalitz plot for $B^o \to \rho\pi \to \pi^+\pi^-\pi^o$ from Snyder and Quinn.

Snyder and Quinn have performed an idealized analysis that uses 1000 or 2000 flavor tagged background free events. The 1000 event sample usually yields good results for $\alpha$, but sometimes does not resolve the ambiguity. With the 2000 event sample, however, they always succeed.

Recently Quinn and Silva have pointed out ways of using time integrated untagged data to specify some of the parameters with larger data samples [41]. Some concern for the effect of the $B^*$ pole on the data has been expressed by Deandrea *et al* [42].

The decay $B^o \to \pi^+\pi^-$ can be used with some theoretical input to resolve the remaining ambiguity in $\sin(2\alpha)$. The difference in CP asymmetries between $\pi\pi$ and $\rho\pi$ is given by

$$a(\pi\pi) - a(\rho\pi) = -2(A_P/A_T)cos(\delta_P - \delta_T)\,[cos(2\alpha)\sin(\alpha)] \quad , \tag{1.50}$$

where $A_P$ and $A_T$ denote the Penguin and Tree amplitudes, respectively, and the $\delta$'s represent their strong phase shifts. Factorization can be used to get the sign of $A_P/A_T$ and the strong phase shifts are believed to be small enough that $\cos(\delta_P - \delta_T)$ is positive [43].

## 1.8 Techniques for Determining $\gamma$

The angle $\gamma$ could in principle be measured using a CP eigenstate of $B_s$ decay that was dominated by the $b \to u$ transition. One such decay that has been suggested is $B_s \to \rho^o K_S$.

However, there are the same "Penguin pollution" problems as in $B^o \to \pi^+\pi^-$, but they are more difficult to resolve in the vector-pseudoscalar final state. (Note, the pseudoscalar-pseudoscalar final state here is $\pi^o K_S$, which does not have a measurable decay vertex.)

Fortunately, there are other ways of measuring $\gamma$. CP eigenstates are not used, which introduces discrete ambiguities. However, combining several methods should remove these. We have studied three methods of measuring $\gamma$.

### 1.8.1 Measurement of $\gamma$ Using Time-Dependent CP violation in $B_s$ Decays

The first method uses the decays $B_s \to D_s^{\pm} K^{\mp}$ where a time-dependent CP violation can result from the interference between the direct decay and the mixing-induced decay [44]. Fig. 1.12 shows the two direct decay processes for $\overline{B}_s^o$.

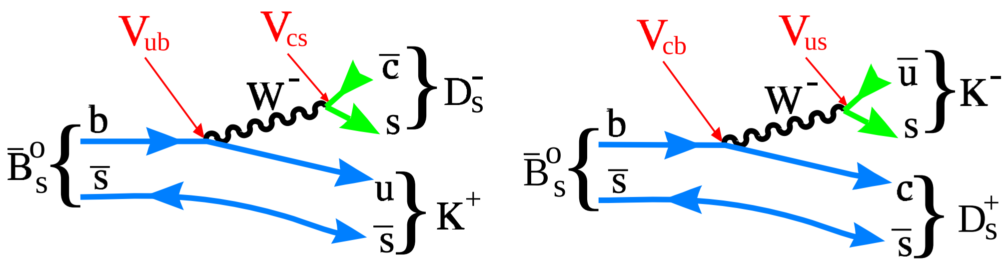


Figure 1.12: Two diagrams for $\overline{B}_s^o \to D_s^{\pm} K^{\mp}$.

Consider the following time-dependent rates that can be separately measured using flavor tagging of the other $b$:

$$\begin{aligned}
\Gamma(B_s \to f) &= |M|^2 e^{-t}\{\cos^2(xt/2) + \rho^2 \sin^2(xt/2) - \rho \sin(\phi + \delta)\sin(xt)\} \\
\Gamma(\bar{B}_s \to \bar{f}) &= |M|^2 e^{-t}\{\cos^2(xt/2) + \rho^2 \sin^2(xt/2) + \rho \sin(\phi - \delta)\sin(xt)\} \\
\Gamma(B_s \to \bar{f}) &= |M|^2 e^{-t}\{\rho^2\cos^2(xt/2) + \sin^2(xt/2) - \rho \sin(\phi - \delta)\sin(xt)\} \\
\Gamma(\bar{B}_s \to f) &= |M|^2 e^{-t}\{\rho^2\cos^2(xt/2) + \sin^2(xt/2) + \rho \sin(\phi + \delta)\sin(xt)\},
\end{aligned} \tag{1.51}$$

where $M = \langle\, f|B\rangle$, $\rho = \frac{\langle\, f|\bar{B}\rangle}{\langle\, f|B\rangle}$, $\phi$ is the weak phase between the 2 amplitudes and $\delta$ is the strong phase between the 2 amplitudes. The three parameters $\rho$, $\sin(\phi+\delta), \sin(\phi-\delta)$ can be extracted from a time-dependent study. If $\rho = O(1)$ the fewest number of events are required.

In the case of $B_s$ decays where $f = D_s^+ K^-$ and $\bar{f} = D_s^- K^+$, the weak phase is $\gamma$.[5] Using this technique $\sin(\gamma)$ is determined with a four-fold ambiguity. If $\Delta\Gamma(B_s)$ is of the order of 10%, then the ambiguities can be resolved.

[5]This is an approximation. The phase is precisely $\gamma - 2\chi + \chi'$, see section 1.9.

### 1.8.2 Measurement of $\gamma$ Using Charged $B$ Decay Rates

Another method for extracting $\gamma$ has been proposed by Atwood, Dunietz and Soni [45], who refined a suggestion by Gronau and Wyler [46]. A large CP asymmetry can result from the interference of the decays $B^- \to K^- D^o, D^o \to f$ and $B^- \to K^- \overline{D}^o, \overline{D}^o \to f$, where $f$ is a doubly-Cabibbo suppressed decay of the $D^o$ (for example $f = K^+\pi^-, K\pi\pi$, etc.). The overall amplitudes for the two decays are expected to be approximately equal in magnitude. (Note that $B^- \to K^- \overline{D}^o$ is color-suppressed and $B^- \to K^- D^0$ is color-allowed.) The weak phase difference between them is $\gamma$. To observe a CP asymmetry there must also be a non-zero strong phase between the two amplitudes. It is necessary to measure the branching ratio $\mathcal{B}(B^- \to K^- f)$ for at least 2 different states $f$ in order to determine $\gamma$ up to discrete ambiguities. Three-body $D^o$ decays are not suggested since the strong $D$ decay phase shifts can vary over the Dalitz plot. Even in quasi-two body decays, such as $K^*\pi$ there may be residual interference effects which could lead to false results. Therefore, the modes that can best be used are $D^o \to K^-\pi^+$ and $K^+K^-$ $(\pi^+\pi^-)$ final states.

We now discuss this method in more detail. Consider a two-body $B^-$ decay into a neutral charmed meson, either a $D^o$ or a $\overline{D}^o$ and a $K^-$. Let us further take the final state of the charmed meson to be a $K^+\pi^-$. There are two sequential decay processes that can lead to this situation, shown in Fig. 1.13. One is where the $B^o$ decays into a $D^o$, that decays in a doubly-Cabibbo suppressed process. The other is where the $B^o$ decays via a $b \to u$ transition to a $D^o$, that decays via a Cabibbo allowed process.

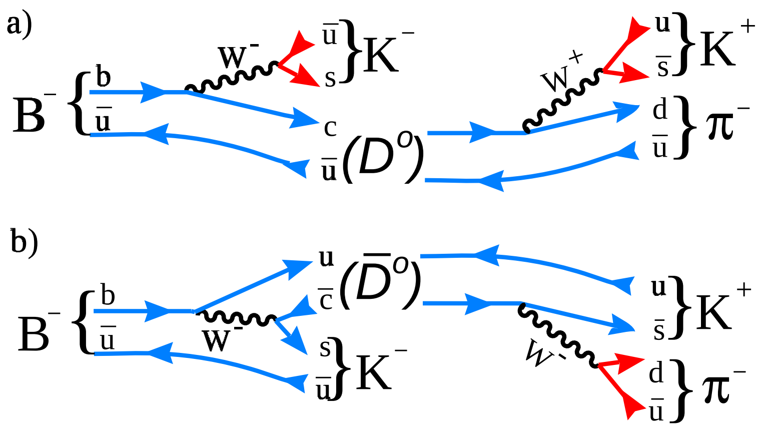


Figure 1.13: Diagrams for the two interfering processes, (a) $B^- \to D^o K^-$ (color allowed) followed by $D^o \to K^+\pi^-$ (doubly-Cabibbo suppressed), and (b) $B^- \to \overline{D}^o K^-$ (color suppressed) followed by $D^o \to K^-\pi^+$ (Cabibbo allowed).

Remarkably, the decay rate for these two processes is quite similar leading to the possibility of large interference effects. Even if the interference effects are not large it is possible to use this method to determine $\gamma$, with some ambiguities. To see how this works, let us define the decay amplitudes and phases in Table 1.3 for two processes, one as described above and the other where the $D^o$ or $\overline{D}^o$ decays into a CP eigenstate. (To be specific, we will take the $K^+K^-$ final state.)

Table 1.3: Amplitudes and Phases for $B^- \to D^o/\overline{D}^o K^-$

| Decay Mode | $B$ Amplitude | $D$ Amplitude | Strong Phase | Weak Phase |
|---|---|---|---|---|
| $B^- \to D^o K^-$, $D^o \to K^+\pi^-$ | $\sqrt{a}$ | $\sqrt{c_d}$ | $\delta_{B1} + \delta_{Cd}$ | 0 |
| $B^- \to \overline{D}^o K^-$, $\overline{D}^o \to K^+\pi^-$ | $\sqrt{b}$ | $\sqrt{c}$ | $\delta_{B2} + \delta_C$ | $\gamma$ |
| $B^- \to D^o K^-$, $D^o \to K^+K^-$ | $\sqrt{a}$ | $\sqrt{c_{CP}}$ | $\delta_{B1} + \delta_{CP}$ | 0 |
| $B^- \to \overline{D}^o K^-$, $\overline{D}^o \to K^-K^+$ | $\sqrt{b}$ | $\sqrt{c_{CP}}$ | $\delta_{B2} + \delta_{CP}$ | $\gamma$ |

All quantities remain the same for the $B^+$ decays, except that the phase $\gamma$ changes sign. The observed decay rates for the four processes can now be calculated by adding and squaring the amplitudes for the same final state. For example, the decay rate for $B^- \to [K^+\pi^-]\, K^-$ (where $[K^+\pi^-]$ denotes a $K^+\pi^-$ pair at the $D^o$ mass), is given by

$$\Gamma(B^- \to \left[K^+\pi^-\right] K^-) = ac_d + bc + 2\sqrt{ac_d bc}\cos(\xi_1 + \gamma) \quad , \tag{1.52}$$

where $\xi_1$ is a combination of $B$ and $D$ phase shifts, $\delta_{B2} - \delta_{B1} + \delta_C - \delta_{Cd}$ and is unknown. Similarly, the decay rates for the other processes are

$$\begin{aligned} \Gamma(B^+ \to \left[K^-\pi^+\right] K^+) &= ac_d + bc + 2\sqrt{ac_d bc}\cos(\xi_1 - \gamma) \\ \Gamma(B^- \to \left[K^+K^-\right] K^-) &= ac_{CP} + bc_{CP} + 2\sqrt{abc_{CP}^2}\cos(\delta_B - \gamma) \\ \Gamma(B^+ \to \left[K^+K^-\right] K^+) &= ac_{CP} + bc_{CP} + 2\sqrt{abc_{CP}^2}\cos(\delta_B + \gamma) \end{aligned} \tag{1.53}$$

where $\delta_B = \delta_{B1} - \delta_{B2}$.

In these four equations, the quantities which are known, or will be precisely known before this measurement is attempted are the decay widths $a$, $c_d$, $c$ and $c_{CP}$. The unknowns are the decay width $b$, two strong phase shifts $\xi_1$ and $\delta_B$ and the weak phase shift $\gamma$. Thus the four equations may be solved for the four unknowns. We can find $\sin\gamma$ with a two-fold ambiguity. If more decay modes are added the ambiguity can be removed. The $B^-$ decay mode can be changed from a $K^-$ to a $K^{*-}$, which could change the strong $B$ decay phase shift, or a different $D^o$ decay mode can be used, such as $K^-\pi^+\pi^+\pi^-$, which would change the strong $D$ decay phase shift. In the latter case, we have to worry about differences in strong phase shifts between $D^o$ and $\overline{D}^o$ due to resonant structure, but use of this mode can shed some information on ambiguity removal.

Comparison of the solutions found here and using $B_s \to D_s^{\pm}K^{\mp}$ as described in the previous section are likely to remove the ambiguities.

### 1.8.3 Measurement of $\gamma$ Using $B \to K\pi$ and $B \to \pi\pi$ Decay Rates and Asymmetries

CLEO has observed the pseudoscalar-pseudoscalar decays $B^o \to K^{\mp}\pi^{\pm}$, $B^- \to K^-\pi^o$, $B^- \to K^o\pi^-$, all with branching ratios around $1.5\times10^{-5}$ and observed or set upper limits on the di-pion final states [34]. Therefore, the Penguin and Tree contributions for $B \to K\pi$ probably do not differ by more than a factor of five, so they can produce observable CP violating effects.

Proposals for extracting information on $\gamma$ have been made using the following experimental ratios:

$$
\begin{aligned}
R &= \frac{\tau(B^+)}{\tau(B^0)}\,\frac{\mathcal{B}(B^0 \to \pi^- K^+) + \mathcal{B}(\bar{B}^0 \to \pi^+ K^-)}{\mathcal{B}(B^+ \to \pi^+ K^0) + \mathcal{B}(B^- \to \pi^- \bar{K}^0)}\,, \\
R_* &= \frac{\mathcal{B}(B^+ \to \pi^+ K^0) + \mathcal{B}(B^- \to \pi^- \bar{K}^0)}{2[\mathcal{B}(B^+ \to \pi^0 K^+) + \mathcal{B}(B^- \to \pi^0 K^-)]}\,,
\end{aligned}
\tag{1.54}
$$

The first, $R$, is by Fleischer and Mannel [48], and the second $R_*$, is by Neubert and Rosner [49], who updated an older suggestion of Gronau and Rosner [50]. The latter paper prompted much theoretical discussion about the effects of isospin conservation and rescattering [51, 52, 53, 54]. A recent paper of Neubert [55] takes into account these criticisms and provides a framework to limit $\gamma$.

More information is obtainable if the CP averaged $\pi^{\pm}\pi^{o}$ branching ratios are also measured, and a CP violating observable defined as

$$
\widetilde{A} \equiv \frac{A_{\rm CP}(\pi^0 K^+)}{R_*} - A_{\rm CP}(\pi^+ K^0) \quad , \tag{1.55}
$$

where for example

$$
A_{\rm CP}(\pi^0 K^+) = \frac{\Gamma(B^+ \to \pi^o K^+) - \Gamma(B^- \to \pi^o K^-)}{\Gamma(B^+ \to \pi^o K^+) + \Gamma(B^- \to \pi^o K^-)} \quad . \tag{1.56}
$$

To summarize Neubert's strategy for determining $\gamma$: From measurements of the CP-averaged branching ratio for the decays $B^{\pm} \to \pi^{\pm}\pi^0$, $B^{\pm} \to \pi^{\pm}K^0$ and $B^{\pm} \to \pi^0 K^{\pm}$, the ratio $R_*$ and a parameter $\bar{\varepsilon}_{3/2}$ are determined. Next, from measurements of the rate asymmetries in the decays $B^{\pm} \to \pi^{\pm}K^0$ and $B^{\pm} \to \pi^0 K^{\pm}$ the quantity $\widetilde{A}$ is determined.

In Fig. 1.14, we show the contour bands as given by Neubert in the $\phi$-$\gamma$ plane. Here $\phi$ is a strong interaction phase-shift. Assuming that $\sin\gamma > 0$ as suggested by the global analysis of the unitarity triangle, the sign of $\widetilde{A}$ determines the sign of $\sin\phi$. In the plot, we assume here that $0^\circ \le \phi \le 180^\circ$. For instance, if $R_* = 0.7$ and $\widetilde{A} = 0.2$, then the two solutions are $(\gamma,\phi) \approx (98^\circ, 25^\circ)$ and $(\gamma,\phi) \approx (153^\circ, 67^\circ)$, only the first of which is allowed by the upper bound $\gamma < 105^\circ$ following from the global analysis of the unitarity triangle shown here (section 1.2 or in [15]). It is evident that the contours are rather insensitive to the rescattering effects. According to Neubert, the combined theoretical uncertainty is of order $\pm10^\circ$ on the extracted value of $\gamma$.

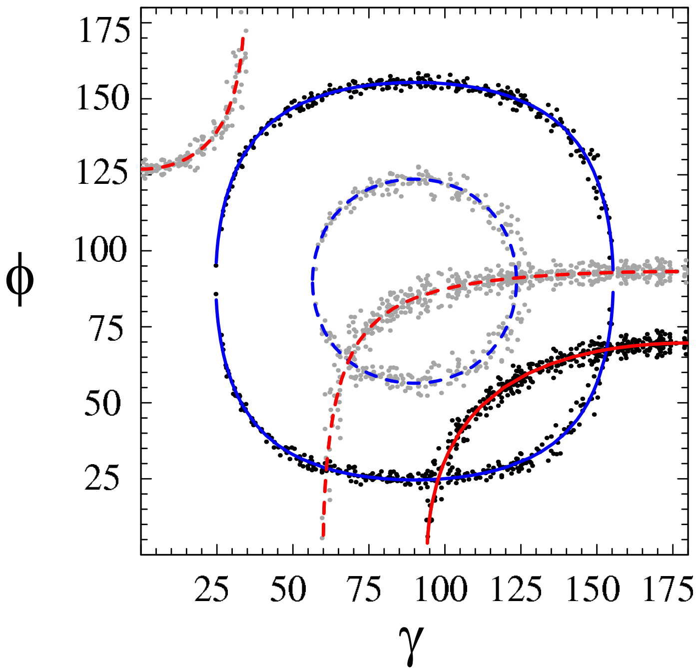


Figure 1.14: Contour plots from Neubert [55] for the quantities $R_*$ ("hyperbolas") and $\widetilde{A}$ ("circles") plotted in the $\phi-\gamma$ plane. The units are degrees. The scatter plots show the results including rescattering effects, while the lines refer to $\varepsilon_a = 0$. The solid curves correspond to the contours for $R_* = 0.7$ and $\widetilde{A} = 0.2$, the dashed ones to $R_* = 0.9$ and $\widetilde{A} = 0.4$.

From the contour plots for the quantities $R_*$ and $\widetilde{A}$ the phases $\gamma$ and $\phi$ can then be extracted up to discrete ambiguities. There are also errors in theoretical parameters that must be accounted for.

### 1.8.4 Measurement of $\gamma$ Using CP Asymmetries in $B^o \to \pi^+\pi^-$ and $B^o_s \to K^+K^-$

Yet another interesting method for determining $\gamma$ has been suggested by Fleischer [56]. The decays $B^o \to \pi^+\pi^-$ and $B^o_s \to K^+K^-$ are related to each other by interchanging all down and strange quarks, which is called $U$-spin flavor symmetry [57]. Both channels can occur via Penguin or singly-Cabibbo suppressed tree levels diagrams, shown in Fig. 1.15.

For $B^o \to \pi^+\pi^-$ the transition amplitude is given by

$$A(B^0_d \to \pi^+\pi^-) = \lambda^{(d)}_u \left(A^u_{\rm cc} + A^u_{\rm pen}\right) + \lambda^{(d)}_c A^c_{\rm pen} + \lambda^{(d)}_t A^t_{\rm pen}\,, \tag{1.57}$$

where $A^u_{\rm cc}$ is due to the tree contributions, and the amplitudes $A^j_{\rm pen}$ describe penguin topologies with internal $j$ quarks ($j \in \{u, c, t\}$). These penguin amplitudes take into account both QCD and electroweak penguin contributions. The quantities

$$\lambda^{(d)}_j \equiv V_{jd}V^*_{jb} \tag{1.58}$$

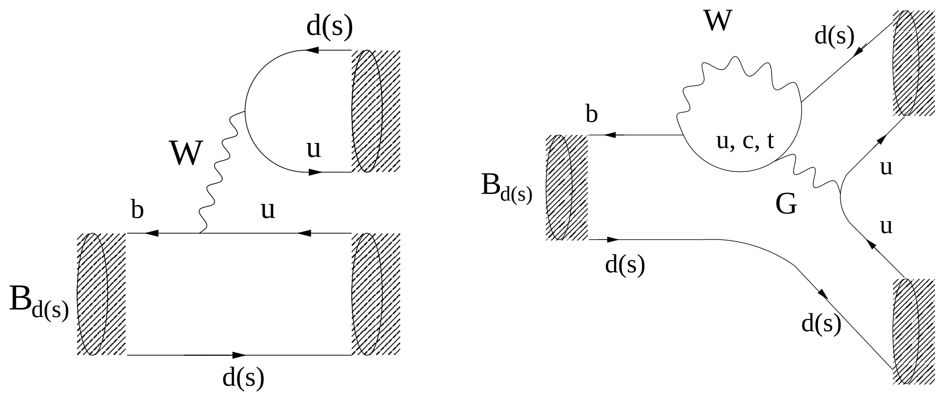


Figure 1.15: Feynman diagrams contributing to $B_d \to \pi^+\pi^-$ and $B_s \to K^+K^-$ (from Fleischer).

are the usual CKM factors. If we make use of the unitarity of the CKM matrix and use the Wolfenstein parameterization, we have

$$A(B_d^0 \to \pi^+\pi^-) = e^{i\gamma}\left(1 - \frac{\lambda^2}{2}\right)\mathcal{C}\left[1 - d\,e^{i\theta}e^{-i\gamma}\right], \tag{1.59}$$

where

$$\mathcal{C} \equiv \lambda^3 A\, R_b\left(A_{\mathrm{cc}}^{u} + A_{\mathrm{pen}}^{ut}\right) \tag{1.60}$$

with $A_{\mathrm{pen}}^{ut} \equiv A_{\mathrm{pen}}^{u} - A_{\mathrm{pen}}^{t}$, and

$$d\,e^{i\theta} \equiv \frac{1}{(1-\lambda^2/2)R_b}\left(\frac{A_{\mathrm{pen}}^{ct}}{A_{\mathrm{cc}}^{u} + A_{\mathrm{pen}}^{ut}}\right). \tag{1.61}$$

The quantity $A_{\mathrm{pen}}^{ct}$ is defined in analogy to $A_{\mathrm{pen}}^{ut}$, and the CKM factors are given by

$$\lambda \equiv |V_{us}| = 0.22\,, \quad A \equiv \frac{1}{\lambda^2}|V_{cb}| \sim 0.8\,, \quad R_b \equiv \frac{1}{\lambda}\left|\frac{V_{ub}}{V_{cb}}\right| \sim 0.4. \tag{1.62}$$

For the following considerations, time-dependent CP asymmetries play a key role. In the case of a general $B_d$ decay into a final CP eigenstate $|f\rangle$, satisfying

$$(\mathcal{CP})|f\rangle = \eta\,|f\rangle, \tag{1.63}$$

where $\eta$ here is not the Wolfenstein parameter, we have (see equation 1.37)

$$\begin{aligned} a_{\mathrm{CP}}(B_d(t) \to f) &\equiv \frac{\Gamma(B_d^0(t) \to f) - \Gamma(\overline{B_d^0}(t) \to f)}{\Gamma(B_d^0(t) \to f) + \Gamma(\overline{B_d^0}(t) \to f)} \\ &= \mathcal{A}_{\mathrm{CP}}^{\mathrm{dir}}(B_d \to f)\cos(\Delta m_d t) + \mathcal{A}_{\mathrm{CP}}^{\mathrm{mix}}(B_d \to f)\sin(\Delta m_d t)\,. \end{aligned} \tag{1.64}$$

For the case of $B^o \to \pi^+\pi^-$, the decay amplitude takes the same form as (1.59), and we obtain the following expressions for the "direct" and "mixing-induced" CP-violating observables:

$$\mathcal{A}_{\rm CP}^{\rm dir}(B_d \to f) = -\left[\frac{2\,d \sin\theta \sin\gamma}{1 - 2\,d\cos\theta\cos\gamma + d^2}\right] \tag{1.65}$$

$$\mathcal{A}_{\rm CP}^{\rm mix}(B_d \to f) = \eta\left[\frac{\sin(2\beta+2\gamma) - 2\,d\,\cos\theta\,\sin(2\beta+\gamma) + d^2\sin 2\beta}{1 - 2\,d\cos\theta\cos\gamma + d^2}\right], \tag{1.66}$$

where $\eta$ is equal to $+1$; for negligible values of the "penguin parameter" $d$, we have $\mathcal{A}_{\rm CP}^{\rm mix}(B_d \to \pi^+\pi^-) = \sin(2\beta+2\gamma) = -\sin(2\alpha)$. However, the penguin contributions are expected to play an important role.

Consider now the decay $B_s^0 \to K^+K^-$. It originates from $\bar{b} \to \bar{u}u\bar{s}$ quark-level processes, as can be seen in Fig. 1.15. Using a notation similar to that in (1.59), we obtain

$$A(B_s^0 \to K^+K^-) = e^{i\gamma}\lambda\,\mathcal{C}'\left[1 + \left(\frac{1-\lambda^2}{\lambda^2}\right) d' e^{i\theta'} e^{-i\gamma}\right], \tag{1.67}$$

where

$$\mathcal{C}' \equiv \lambda^3 A\,R_b\left(A_{\rm cc}^{u'} + A_{\rm pen}^{ut'}\right) \tag{1.68}$$

and

$$d' e^{i\theta'} \equiv \frac{1}{(1-\lambda^2/2)R_b}\left(\frac{A_{\rm pen}^{ct'}}{A_{\rm cc}^{u'} + A_{\rm pen}^{ut'}}\right) \tag{1.69}$$

correspond to (1.60) and (1.61), respectively. The primes remind us that we are dealing with a $\bar{b} \to \bar{s}$ transition. It should be emphasized that (1.59) and (1.67) are completely general parameterizations of the $B_d^0 \to \pi^+\pi^-$ and $B_s^0 \to K^+K^-$ decay amplitudes within the Standard Model, relying only on the unitarity of the CKM matrix. In particular, these expressions take into account also final-state interaction effects, which can be considered as long-distance penguin topologies with internal up- and charm-quark exchanges.

There may be a sizeable width difference $\Delta\Gamma_s \equiv \Gamma_{\rm H}^{(s)} - \Gamma_{\rm L}^{(s)}$ between the $B_s$ mass eigenstates [58], which may allow studies of CP violation with "untagged" $B_s$ data samples [23]. Such untagged rates take the following form:

$$\Gamma(B_s^0(t) \to f) + \Gamma(\overline{B_s^0}(t) \to f) \propto R_{\rm H}\,e^{-\Gamma_{\rm H}^{(s)}t} + R_{\rm L}\,e^{-\Gamma_{\rm L}^{(s)}t}, \tag{1.70}$$

whereas the time-dependent CP asymmetry is given by

$$\begin{aligned} a_{\rm CP}(B_s(t) \to f) &\equiv \frac{\Gamma(B_s^0(t) \to f) - \Gamma(\overline{B_s^0}(t) \to f)}{\Gamma(B_s^0(t) \to f) + \Gamma(\overline{B_s^0}(t) \to f)} \\ &= 2\,e^{-\Gamma_s t}\left[\frac{\mathcal{A}_{\rm CP}^{\rm dir}(B_s \to f)\cos(\Delta m_s t) + \mathcal{A}_{\rm CP}^{\rm mix}(B_s \to f)\sin(\Delta m_s t)}{e^{-\Gamma_{\rm H}^{(s)}t} + e^{-\Gamma_{\rm L}^{(s)}t} + \mathcal{A}_{\Delta\Gamma}(B_s \to f)\left(e^{-\Gamma_{\rm H}^{(s)}t} - e^{-\Gamma_{\rm L}^{(s)}t}\right)}\right] \end{aligned} \tag{1.71}$$

with $\mathcal{A}_{\Delta\Gamma}(B_s \to f) = (R_{\rm H} - R_{\rm L})/(R_{\rm H} + R_{\rm L})$. If the $B_s^0 \to f$ decay amplitude takes the same form as (1.67), we have

$$\mathcal{A}_{\rm CP}^{\rm dir}(B_s \to f) = + \left[ \frac{2\,\tilde{d}' \sin\theta' \sin\gamma}{1 + 2\,\tilde{d}' \cos\theta' \cos\gamma + \tilde{d}'^2} \right] \tag{1.72}$$

$$\mathcal{A}_{\rm CP}^{\rm mix}(B_s \to f) = +\eta \left[ \frac{\sin(2\chi + 2\gamma) + 2\,\tilde{d}' \,\cos\theta' \,\sin(2\chi + \gamma) + \tilde{d}'^2 \sin 2\chi}{1 + 2\,\tilde{d}' \cos\theta' \cos\gamma + \tilde{d}'^2} \right] \tag{1.73}$$

$$\mathcal{A}_{\Delta\Gamma}(B_s \to f) = -\,\eta \left[ \frac{\cos(2\chi + 2\gamma) + 2\,\tilde{d}' \cos\theta' \cos(2\chi + \gamma) + \tilde{d}'^2 \cos 2\chi}{1 + 2\,\tilde{d}' \cos\theta' \cos\gamma + \tilde{d}'^2} \right]. \tag{1.74}$$

These observables are not independent quantities, and satisfy the relation

$$\left[\mathcal{A}_{\rm CP}^{\rm dir}(B_s \to f)\right]^2 + \left[\mathcal{A}_{\rm CP}^{\rm mix}(B_s \to f)\right]^2 + \left[\mathcal{A}_{\Delta\Gamma}(B_s \to f)\right]^2 = 1. \tag{1.75}$$

In the general expressions (1.72)–(1.74), we have introduced the abbreviation

$$\tilde{d}' \equiv \left(\frac{1 - \lambda^2}{\lambda^2}\right) d', \tag{1.76}$$

and $2\chi = 2\arg(V_{ts}^* V_{tb})$ denotes the $B_s^o$–$\overline{B_s^o}$ mixing phase. Within the Standard Model, we have $2\chi \approx 0.03$ due to a Cabibbo suppression of $\mathcal{O}(\lambda^2)$, implying that $2\chi$ is very small. This phase can be determined using $B_s \to J/\psi\,\eta'$ decays (see section 1.9).

Since the decays $B_d \to \pi^+\pi^-$ and $B_s \to K^+K^-$ are related to each other by interchanging all strange and down quarks, the $U$-spin flavor symmetry of strong interactions implies

$$d' = d \tag{1.77}$$

$$\theta' = \theta. \tag{1.78}$$

In contrast to certain isospin relations, electroweak penguins do not lead to any problems in the $U$-spin relations (1.77) and (1.78), according to Fleischer.

In general we have five physics quantities of interest, $2\chi$, $d$, $\theta$, $2\beta$ and $\gamma$. Let us now assume that $\sin(2\beta)$ will be measured and $\sin(2\chi)$ either measured or tightly limited. Only $d$, $\theta$ and $\gamma$ then need to be determined.

We have four possible measured quantities provided by the time-dependent CP asymmetries of the modes $B_d \to \pi^+\pi^-$ and $B_s \to K^+K^-$. These four quantities are $\mathcal{A}_{\rm CP}^{\rm mix}(B_s \to K^+K^-)$, $\mathcal{A}_{\rm CP}^{\rm mix}(B_d \to \pi^+\pi^-)$, $\mathcal{A}_{\rm CP}^{\rm dir}(B_s \to K^+K^-)$ and $\mathcal{A}_{\rm CP}^{\rm dir}(B_d \to \pi^+\pi^-)$. To implement this plan we need measure only 3 of these four quantities, or combinations of them. For example, it may be difficult to independently determine $\mathcal{A}_{\rm CP}^{\rm mix}(B_d \to \pi^+\pi^-)$ and $\mathcal{A}_{\rm CP}^{\rm dir}(B_d \to \pi^+\pi^-)$, because of the small number of observable $B^o$ oscillations before the exponential decay reduces the number of events too much. However, the sum

$$\begin{aligned} a_{CP}^{\pi^+\pi^-} &= \int_0^\infty \mathcal{A}_{\rm CP}^{\rm dir} \cos(\Delta m_d t) + \mathcal{A}_{\rm CP}^{\rm mix} \sin(\Delta m_d t) \\ &= \frac{1}{1 + x^2} \mathcal{A}_{\rm CP}^{\rm dir} + \frac{x}{1 + x^2} \mathcal{A}_{\rm CP}^{\rm mix} \end{aligned} \tag{1.79}$$

can be determined and used with the other two measurements from $B_s^o \to K^+K^-$. Clearly other scenarios are possible.

### 1.8.5 Opportunities with $B_s$ Mesons if $\Delta\Gamma$ is ~10%

Measurement of $\Delta\Gamma$ can be used to estimate in an interesting but model dependent manner the value of $\Delta m_s$ and thus provides a redundant check on $B_s$ mixing measurements [23].

Should a large enough $\Delta\Gamma$ be determined there exist other possible ways to determine some of the interesting physics quantities discussed above. Some of these studies can be done without flavor tagging. In fact, the time evolution of untagged observables for a $B_s$ decay into a vector-vector final state is proportional to

$$\left(e^{-\Gamma_H t} - e^{-\Gamma_L t}\right) \sin\phi_{CKM}, \tag{1.80}$$

where $\phi_{CKM}$ is a CP violating angle from the CKM matrix and depends on the specific decay mode.

In general the angular distribution for $B_s \to VV$ is expressed in terms of transversity in a manner similar to equation 1.46, with the major difference being that the angular variables are time dependent. The time evolution of the decay $B_s \to J/\psi\phi$ is given in Table 1.4 [59].

| Observable | Time evolution |
|---|---|
| $\lvert A_0(t)\rvert^2$ | $\lvert A_0(0)\rvert^2 \left[e^{-\Gamma_L t} - e^{-\overline{\Gamma} t}\sin(\Delta m t)\sin(2\chi)\right]$ |
| $\lvert A_\parallel(t)\rvert^2$ | $\lvert A_\parallel(0)\rvert^2 \left[e^{-\Gamma_L t} - e^{-\overline{\Gamma} t}\sin(\Delta m t)\sin(2\chi)\right]$ |
| $\lvert A_\perp(t)\rvert^2$ | $\lvert A_\perp(0)\rvert^2 \left[e^{-\Gamma_H t} + e^{-\overline{\Gamma} t}\sin(\Delta m t)\sin(2\chi)\right]$ |
| $\mathrm{Re}(A_0^*(t)A_\parallel(t))$ | $\lvert A_0(0)\rvert\lvert A_\parallel(0)\rvert\cos(\delta_2-\delta_1)\left[e^{-\Gamma_L t} - e^{-\overline{\Gamma} t}\sin(\Delta m t)\sin(2\chi)\right]$ |
| $\mathrm{Im}(A_\parallel^*(t)A_\perp(t))$ | $\lvert A_\parallel(0)\rvert\lvert A_\perp(0)\rvert\left[e^{-\overline{\Gamma} t}\sin(\delta_1 - \Delta m t) + \frac{1}{2}\left(e^{-\Gamma_H t} - e^{-\Gamma_L t}\right)\cos(\delta_1)\sin(2\chi)\right]$ |
| $\mathrm{Im}(A_0^*(t)A_\perp(t))$ | $\lvert A_0(0)\rvert\lvert A_\perp(0)\rvert\left[e^{-\overline{\Gamma} t}\sin(\delta_2 - \Delta m t) + \frac{1}{2}\left(e^{-\Gamma_H t} - e^{-\Gamma_L t}\right)\cos(\delta_2)\sin(2\chi)\right]$ |

Table 1.4: Time evolution of the decay $B_s \to J/\psi(\to l^+l^-)\phi(\to K^+K^-)$ of an initially (i.e. at $t=0$) pure $B_s$ meson. $\delta_{1,2}$ are strong phase shifts.

Combining with the decay of the $\overline{B}_s$ the time evolution of the untagged sample is given by

$$\frac{d^3\Gamma(J/\psi(\to l^+l^-)\phi(\to K^+K^-))}{d\cos\theta\; d\varphi\; d\cos\psi} \propto \frac{9}{16\pi}\Big[\; 2|A_0(0)|^2 e^{-\Gamma_L t}\cos^2\psi(1-\sin^2\theta\cos^2\varphi)$$

$$+\sin^2\psi\{|A_{\|}(0)|^2 e^{-\Gamma_L t}(1-\sin^2\theta\sin^2\varphi)+|A_\perp(0)|^2 e^{-\Gamma_H t}\sin^2\theta\}$$
$$+\frac{1}{\sqrt{2}}\sin 2\psi\left\{|A_0(0)||A_{\|}(0)|\cos(\delta_2-\delta_1)e^{-\Gamma_L t}\sin^2\theta\sin 2\varphi\right\}$$
$$+\left\{\frac{1}{\sqrt{2}}|A_0(0)||A_\perp(0)|\cos\delta_2\sin 2\psi\sin 2\theta\cos\varphi\right.$$
$$\left.-|A_{\|}(0)||A_\perp(0)|\cos\delta_1\sin^2\psi\sin 2\theta\sin\varphi\right\}\frac{1}{2}\left(e^{-\Gamma_H t}-e^{-\Gamma_L t}\right)\delta\phi\Bigg] \quad . \tag{1.81}$$

Thus a study of the time dependent angular distributions can lead to a measurement of $\sin(2\chi)$, especially if $\Delta\Gamma$ is determined before hand. It is also possible to integrate over two of the angles if statistics is limited. The distribution in $J/\psi$ decay angle can be written as

$$\frac{d\Gamma(t)}{d\cos\theta}\propto(|A_0(t)|^2+|A_{\|}(t)|^2)\frac{3}{8}(1+\cos^2\theta)+|A_\perp(t)|^2\ \frac{3}{4}\sin^2\theta \tag{1.82}$$

where the CP violating angle originates from the imaginary parts of the interference terms in the $A$'s.

Other final states have been suggested that provide a measurement of $\gamma$ using the above ideas. One particularly interesting set of decays is $B_s\to K^{*+}K^{*-}$ and $B_s\to K^{*o}\bar{K}^{*o}$ [60].

Finally, it is important to realize that determination of a non-zero $\Delta\Gamma$ allows the measurement of $Re\left(\frac{q}{p}\cdot\frac{\bar{A}}{A}\right)$, that in turn allows the removal of the ambiguities in the CKM angle of interest [23]. For the $B_s$ decays mentioned here this could be $\gamma$ or $\chi$.

## 1.9 Summary of CKM Tests

Our goal is to measure separately the four angles $\alpha$, $\beta$, $\gamma$ and $\chi$. To extract the angles we will measure usually either the $\sin(2\phi)$ or the $\sin\phi$ which leads to discrete *ambiguities* in the determination of $\phi$.

For example, any determination of $\sin(2\phi)$, where $\phi$ is any angle found using the interference of a single decay amplitude with a mixing amplitude has a four-fold ambiguity, where $\phi$, $\pi/2-\phi$, $\pi+\phi$, $3\pi/2-\phi$ are all allowed solutions. One may take the point of view that we know that $\eta$ is a positive quantity and thus we can eliminate two of the four possibilities. However, this would be dangerous in that it could lead to our missing new physics. The only evidence that $\eta$ is positive arises from the measurements of $\epsilon$ and $\epsilon'$ and the fact that theoretical calculations give $B_K>0$ for $\epsilon$. Even accepting that $K_L$ decays give $\eta>0$, it would be foolhardy to miss new physics just because we now assume that $\eta$ must be positive rather than insisting on a clean resolution of the ambiguities that could show a contradiction.

Each of these four angles can be measured most easily using the modes listed in Table 1.5 Other modes which also may turn out to be useful include $B^o\to D^{*+}\pi^-$ and its charge-

Table 1.5: Primary modes useful for measuring CP asymmetries for different CKM angles

| Decay Mode | Angle |
|---|---|
| $B^o \to J/\psi K_S$ | $\sin(2\beta)$ |
| $B^o \to \rho\pi \to \pi^+\pi^-\pi^o$ | $\sin(2\alpha)$ |
| $B_s^o \to D_s^{\mp} K^{\pm}$ | $\sin\gamma$ |
| $B^- \to \overline{D^o} K^-$, and c.c. | $\sin\gamma$ |
| $B_s \to J/\psi\eta'$ | $\sin(2\chi)$ |

conjugate [61], which measures $\sin(-2\beta-\gamma)$ albeit with a small $\approx$1% predicted asymmetry,[6] and $B \to K\pi$ modes which can be used to find $\gamma$ albeit with theoretical uncertainties.

There are three alternative ways to measure $\gamma$, discussed in section 1.8, which serve both to remove ambiguities and perform checks. It will be much more difficult to find other modes to check $\alpha$, however. One approach is to measure the CP asymmetry in $B^o \to \pi^+\pi^-$ and use theoretical models to estimate the effects of Penguin pollution. Minimally, a great deal would be learned about the models. It also turns out that the third ambiguity in $\alpha$ can be removed by comparing the CP violating asymmetry in $\pi^+\pi^-$ with that found in $\rho\pi$ and using some mild theoretical assumptions [43]. After the three angles $\alpha$, $\beta$ and $\gamma$ have been measured, we need to check if they add up to $180^o$. A discrepancy here would show new physics. To be sure, this check is not complete if ambiguities have not been removed. (Even if the angles sum to $180^o$, new physics could hide.)

We also want to measure as precisely as possible the side of the **bd** triangle (see Fig. 1.4) that requires a precise measurement of $B_s$ mixing [63]. The other side is proportional to the magnitude of $V_{ub}$. This will no doubt be measured by $e^+e^-$ $b$-factories and the precision will be limited by theoretical concerns if form-factors in the exclusive decays and $q^2$ distributions in the inclusive decays have been decisively measured.

New physics can add differently to the phases in different decay modes if it contributes differently to the relative decay amplitudes $A/\overline{A}$. Therefore it is interesting to measure CP violation in redundant modes. For example, the decay $B^o \to \phi K_S$ should also measure $\sin(2\beta)$. If it is different than that obtained by $B^o \to J/\psi K_S$, that would be a strong indication of new physics [64]. We list in Table 1.6 other interesting modes to check $\sin(2\beta)$. The branching ratios listed with errors have been measured [65, 66], while those without are theoretical estimates.

Silva and Wolfenstein [67] following Aleksan, Kayser and London [8] argue that the best way to reveal the presence of new physics is to measure $\chi$ and two of $\alpha$, $\beta$ and $\gamma$ and compare with magnitudes of some CKM elements. Recall, in the six CKM triangles in Fig. 1.1, there are four and only four independent phases. Since the angles $\alpha$, $\beta$ and $\gamma$, when properly measured must add to $180^o$, Silva and Wolfenstein take only two of them as independent. The angles $\beta$ and $\gamma$ are expected to be large in the Standard Model. $\chi$ is expected to be of

[6]To measure a CP asymmetry this way requires using equations 1.51, and extracting the strong phase, amplitude ratio, and a small asymmetry: a very difficult task.

Table 1.6: Other modes useful for cross-checking $\sin(2\beta)$

| Decay Mode | Branching Ratio |
|---|---|
| $B^o \to \phi K_S$ | $(0.04 - 1.5) \times 10^{-5}$ |
| $B^o \to D^+ D^-$ | $\approx 10^{-3}$ |
| $B^o \to D^{*+} D^-$ | $\approx 10^{-3}$ |
| $B^o \to \eta' K^o$, | $(5.9 \pm 1.9) \times 10^{-5}$ |
| $B^o \to J/\psi(\pi^o,\ \eta \text{ or } \eta')$ | $(3.4 \pm 1.6) \times 10^{-5}$ |

the order $2\lambda^2\eta \sim 0.02$ and $\chi'$ of the order 0.003.

There is no direct way of measuring the small angle $\chi'$. However the angle $\chi$ can be measured by using $B_s$ decays. The most direct way is to measure the time dependent CP violation caused by the mixing of interference and decay in the modes $B_s \to J/\psi\eta$, $\eta \to \gamma\gamma$, or $B_s \to J/\psi\eta'$, $\eta' \to \rho^o\gamma$. The time resolution has to be excellent in order to resolve the fast $B_s$ oscillations. The all-charged mode $B_s \to J/\psi\phi$ can also be used [59], but this requires a complicated angular analysis and consequently a great deal of data.

Let us try and get some idea of the sizes of the angles $\alpha$, $\beta$ and $\gamma$. The expected range of angles derived from Fig. 1.4 is shown in Fig. 1.16. These plots show only the most likely

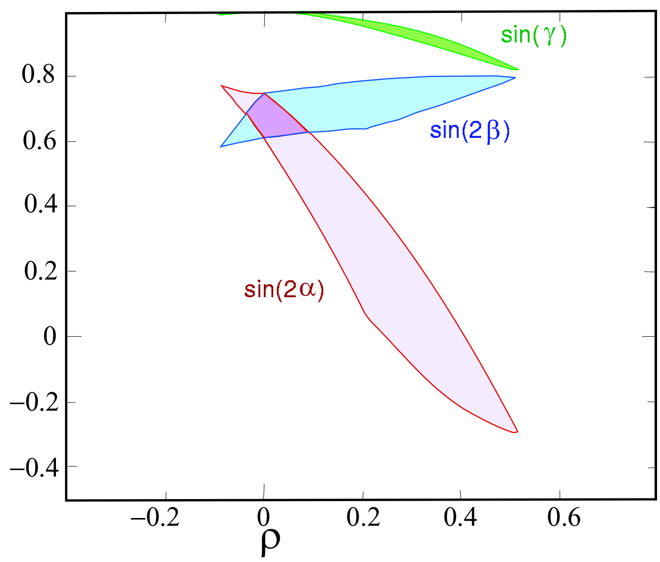


Figure 1.16: The "allowed" values for the three angles of the CKM triangle derived from the allowed, i.e. $1\sigma$ overlap, region of Fig. 1.4.

values in the Standard Model. Recall that they are based on the overlap of $\pm 1\sigma$ bands from constraints on $V_{ub}/V_{cb}$, $\epsilon$, and $B_d$ mixing. However, this gives us a good indication on where we should target our measuring potential. The angle $\chi$ as mentioned previously is expected to be small $\approx 2\lambda^2\eta$.

Measurements of the magnitudes of CKM matrix elements all come with theoretical errors. Some of these are hard to estimate. We now try and view realistically how to combine CP violating phase measurements with the magnitude measurements to best test the Standard Model.

The best measured magnitude is that of $|V_{us}/V_{ud}| = \lambda = 0.2205 \pm 0.0018$, where the quoted error has approximately equal experimental and theoretical contributions [11]. Silva and Wolfenstein [67], along with Aleksan, Kayser and London [8] show that the Standard Model can be checked in a profound manner by seeing if:

$$\sin\chi = \left|\frac{V_{us}}{V_{ud}}\right|^2 \frac{\sin\beta\ \sin\gamma}{\sin(\beta+\gamma)} \quad . \tag{1.83}$$

Here the precision of the check is limited by the measurement of $\sin\chi$, not of $\lambda$. This check is likely to reveal if new physics is present, even if other checks have not shown new physics. The example given by Silva and Wolfenstein [67] is a new phase added to the Standard Model mixing phase, which is missed in the measurement of $\alpha$ plus $\beta$ since it cancels in the sum. Two other checks can be performed, which have similar structures.

$$\sin\chi = \left|\frac{V_{ub}}{V_{cb}}\right|^2 \frac{\sin\gamma\ \sin(\beta+\gamma)}{\sin\beta} \quad , \tag{1.84}$$

$$\sin\chi = \left|\frac{V_{td}}{V_{ts}}\right|^2 \frac{\sin\beta\ \sin(\beta+\gamma)}{\sin\gamma} \quad . \tag{1.85}$$

Note that it is, in principle, possible to determine the magnitudes of $|V_{ub}/V_{cb}|$ and $|V_{td}/V_{ts}|$, just by measuring the angles precisely enough. This is true because of the unitarity of the CKM matrix.

Before these precision tests can be carried out, it will be useful to check the consistency of the measurements of $\epsilon$ in $K_L$ decay, $|V_{ub}/V_{cb}|$ from semileptonic $b$ decay and the ratio of $x_s/x_d$, $B_s/B_d$ mixing parameters. The accuracy of the $\rho-\eta$ constraint from $\epsilon$ is currently determined mostly by $V_{cb}$ and the parameter $B_K$, which can only be calculated not measured. While the determination of $V_{cb}$ will improve in the next several years before it is limited by theoretical errors, the accuracy of $B_K$ will probably not improve, and it will remain difficult to assign a well defined error. Thus, the allowed band in $\epsilon$ will shrink somewhat, but it will remain relatively broad.

$B_s$ mixing may as yet be measured by SLD or CDF. If the oscillations prove to be fast enough, BTeV will make the first measurement. In either case, the ultimate utility of the measurement in restricting the region of the $\rho-\eta$ plane will be determined by the accuracy of the calculation of the ratio $f_{B_d}^2 B_{B_d}/f_{B_s}^2 B_{B_s}$, after the measurement of $x_s$ becomes accurate enough. These parameters have been and are being calculated on the lattice. The accuracy in the above ratio is estimated not to be better than about 10% [68].

The ultimate error on $|V_{ub}|$ will also be theoretical in origin. Experimental measurements from $e^+e^-$ $B$ factories will perform extensive measurements of inclusive semileptonic $b \to u\ell\nu$ decays as well as exclusive decays to the $\pi\ell\nu$ and $\rho\ell\nu$ decays. The form-factors as well as the branching ratios will be measured and should help to restrict the models. However, at this time there isn't a compelling theoretical framework such as HQET for $b \to c\ell\nu$. Thus, we estimate the theoretical error to be currently on the order of $\pm 14\%$, and hope for further improvements.

Thus the intersection of the mixing ratio band with the $V_{ub}$ band should provide a crossing point with reasonable errors. The measurement of each of the individual angles, $\alpha$, $\beta$ and $\gamma$ will need to be consistent within the error band, otherwise the Standard Model will be violated.

## 1.10 Rare Decays as Probes beyond the Standard Model

Rare decays have loops in the decay diagrams which makes them sensitive to high mass gauge bosons and fermions. Thus, they are sensitive to new physics. However, it must be kept in mind that any new effect must be consistent with already measured phenomena such as $B_d^o$ mixing and $b \to s\gamma$.

These processes are often called "Penguin" processes, for unscientific reasons [69]. A Feynman loop diagram is shown in Fig. 1.17 that describes the transition of a $b$ quark into a charged -1/3 $s$ or $d$ quark, which is effectively a neutral current transition. The dominant charged current decays change the $b$ quark into a charged +2/3 quark, either $c$ or $u$.

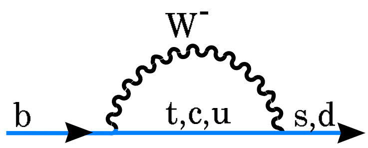


Figure 1.17: Loop or "Penguin" diagram for a $b \to s$ or $b \to d$ transition.

The intermediate quark inside the loop can be any charge +2/3 quark. The relative size of the different contributions arises from different quark masses and CKM elements. For $b \to s$, in terms of the Cabibbo angle ($\lambda$=0.22), we have for $t$:$c$:$u$ - $\lambda^2$:$\lambda^2$:$\lambda^4$. The mass dependence favors the $t$ loop, but the amplitude for $c$ processes can be quite large $\approx$30%. Moreover, as pointed out by Bander, Silverman and Soni [70], interference can occur between $t$, $c$ and $u$ diagrams and lead to CP violation. In the Standard Model it is not expected to occur when $b \to s$, due to the lack of a CKM phase difference, but could occur when $b \to d$. In any case, it is always worth looking for this effect; all that needs to be done, for example, is to compare the number of $K^{*-}\gamma$ events with the number of $K^{*+}\gamma$ events.

There are other possibilities for physics beyond the Standard Model to appear. For example, the $W^-$ in the loop can be replaced by some other charged object such as a Higgs; it is also possible for a new object to replace the $t$.

### 1.10.1 $b \to s\gamma$

This process occurs when any of the charged particles in Fig. 1.17 emits a photon. CLEO first measured the inclusive rate [71] as well as the exclusive rate into $K^*(890)\gamma$ [72]. There is an updated CLEO measurement [73] using 1.5 times the original data sample and a new measurement from ALEPH [74].

To remove background CLEO used two techniques originally, one based on "event shapes" and the other on summing exclusively reconstructed $B$ samples. CLEO uses eight different shape variables [71], and defines a variable $r$ using a neural network to distinguish signal from background. The idea of the $B$ reconstruction analysis is to find the inclusive branching ratio by summing over exclusive modes. The allowed hadronic system is composed of either a $K_S \to \pi^+\pi^-$ candidate or a $K^\mp$ combined with 1-4 pions, only one of which can be neutral. The restriction on the number and kind of pions maximizes efficiency while minimizing background. It does however lead to a model dependent error. Then both analysis techniques are combined. Currently, most of the statistical power of the analysis (~80%) comes from summing over the exclusive modes.

Fig. 1.18 shows the photon energy spectrum of the inclusive signal, compared with the model of Ali and Greub [75]. A fit to the model over the photon energy range from 2.1 to 2.7 GeV/c gives the branching ratio result shown in Table 1.7, where the first error is statistical and the second systematic.

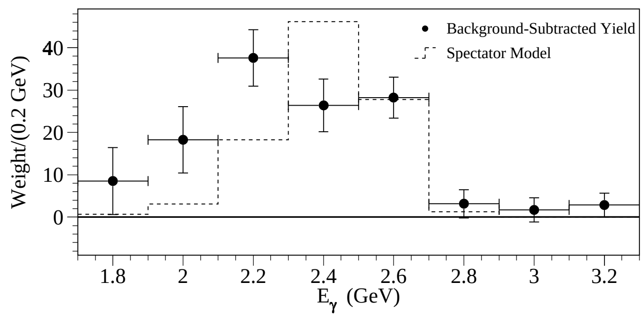


Figure 1.18: The background subtracted photon energy spectrum from CLEO. The dashed curve is a spectator model prediction from Ali and Greub.

Table 1.7: Experimental results for $b \to s\gamma$

| Sample | branching ratio |
|---|---|
| CLEO | $(3.15 \pm 0.35 \pm 0.41) \times 10^{-4}$ |
| ALEPH | $(3.11 \pm 0.80 \pm 0.72) \times 10^{-4}$ |
| Average | $(3.14 \pm 0.48) \times 10^{-4}$ |
| Theory[76] | $(3.28 \pm 0.30) \times 10^{-4}$ |

ALEPH reduces the backgrounds by weighting candidate decay tracks in a $b \to s\gamma$ event by a combination of their momentum, impact parameter with respect to the main vertex and rapidity with respect to the $b$-hadron direction [74]. Their result is shown in Table 1.7. The world average experimental value is also given, as well as the theoretical prediction.

The Standard Model prediction is in good agreement with the data.

Hewett has given a good review of the many minimal supergravity models which are excluded by the data [77]. Improved experimental and theoretical accuracy are required to move beyond the Standard Model here. A measurement of $b \to d\gamma$ would be most interesting.

Triple gauge boson couplings are of great interest in checking the standard model. If there were an anomalous $WW\gamma$ coupling it would serve to change the Standard Model rate. $p\bar{p}$ collider experiments have also published results limiting such couplings [78]. In a two-dimensional space defined by $\Delta\kappa$ and $\lambda$, the D0 constraint appears as a tilted ellipse and the $b \to s\gamma$ as nearly vertical bands. In the standard model both parameters are zero.

### 1.10.2 The Exclusive Decays $K^*\gamma$ and $\rho\gamma$

The exclusive branching ratio is far more difficult to predict than the inclusive. CLEO measures $\mathcal{B}(B \to K^*(890)\gamma) = (4.2 \pm 0.8 \pm 0.6) \times 10^{-5}$, with this exclusive final state comprising $(18 \pm 7)\%$ of the total $b \to s\gamma$ rate [79].

CLEO also limits $\mathcal{B}(B \to \rho\gamma) < 1.2 \times 10^{-5}$ at 90% confidence level [79]. This leads to a model dependent limit on $|V_{td}/V_{ts}|^2 < 0.45 - 0.56$, which is not very significant. It may be possible that improved measurements can find a meaningful limit, although that has been disputed [80].

### 1.10.3 $b \to s\ell^+\ell^-$

The diagrams that contribute to $b \to s\ell^+\ell^-$, where $\ell$ refers to either an electron or muon are shown in Fig. 1.19.

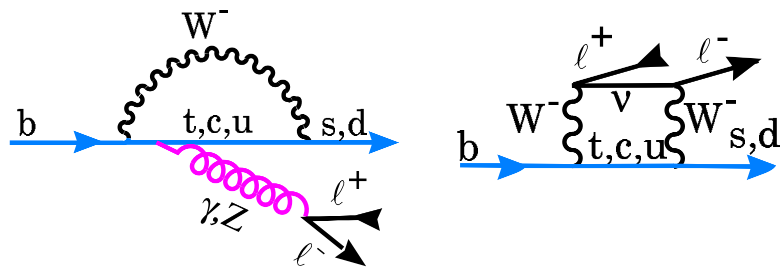


Figure 1.19: Loop or "Penguin" diagram for a $b \to s\ell^+\ell^-$ transition.

Since more diagrams contribute here than in $b \to s\gamma$, different physics can be probed. CP violation can be looked at in both the branching ratios and the polarization of the lepton pair [81]. No signals have been seen as yet in any inclusive or exclusive modes. When searching for such decays, care must be taken to eliminate the mass region in the vicinity of the $J/\psi$

Table 1.8: Searches for $b \to s\ell^+\ell^-$ decays

| $b$ decay mode | 90% c.l. upper limit | Group | Ali *et al* Prediction [82] |
|---|---|---|---|
| $s\mu^+\mu^-$ | $50 \times 10^{-6}$ | UA1 [83] | $(8 \pm 2) \times 10^{-6}$ |
| | $5.7 \times 10^{-6}$ | CLEO [84] | |
| $K^{*o}\mu^+\mu^-$ | $4.0 \times 10^{-6}$ | CDF [85] | $2.9 \times 10^{-6}$ |
| | $23 \times 10^{-6}$ | UA1 [83] | |
| | $9.5 \times 10^{-6}$ | CLEO [84] | |
| $K^{*o}e^+e^-$ | $13 \times 10^{-6}$ | CLEO [84] | $5.6 \times 10^{-6}$ |
| $K^-\mu^+\mu^-$ | $9.7 \times 10^{-6}$ | CLEO [84] | $0.6 \times 10^{-6}$ |
| | $5.2 \times 10^{-6}$ | CDF [85] | |
| $K^-e^+e^-$ | $2.5 \times 10^{-6}$ | CLEO [84] | $0.6 \times 10^{-6}$ |

or $\psi'$ resonances, lest these more prolific processes, that are not rare decays, contaminate the sample. The results of searches are shown in Table 1.8.

BTeV has the ability to search for both exclusive and inclusive dilepton final states. The inclusive measurement can be done following the techniques used by CLEO to discover inclusive $b \to s\gamma$ and set upper limits on $b \to s\ell^+\ell^-$. CLEO doesn't have vertex information, so they choose track combinations assigning a kaon hypothesis to one track and pion hypotheses to the other charged tracks. They allow up to four pions, only one of which can be neutral and proceed to reconstruct each combination as if it were an exclusive decay mode. If any combination succeeds, they keep it. BTeV can improve on this procedure in two ways. First of all BTeV will have RICH $K\pi$ separation. Secondly we can insist that the charged particles are consistent with coming from a $b$ decay vertex. Of course, we lose the power of the beam energy constraint that is so efficient at rejecting background at the $\Upsilon(4S)$. However, it is a detailed question as to whether or not we more than make up the rejection power by using our advantages.

$B$'s can also decay into dilepton final states. The Standard Model diagrams are shown in Fig. 1.20. In (a) the decay rate is proportional to $|V_{ub}|^2 f_B^2$. The diagram in (b) is much larger for $B_s$ than $B_d$, again the factor of $|V_{ts}/V_{td}|^2$. Results of searches are given in Table 1.9.

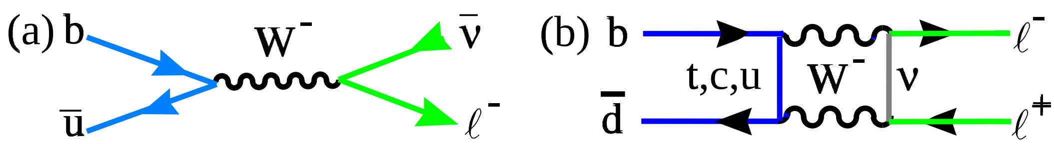


Figure 1.20: Decay diagrams resulting in dilepton final states. (a) is an annihilation diagram, and (b) is a box diagram.

Searches for rare decays modes make up an important part of the BTeV physics program.

Table 1.9: Upper limits on $b \to$ dilepton decays (@90% c.l.)

| | $\mathcal{B}(B^o \to \ell^+\ell^-)$ | | $\mathcal{B}(B_s \to \ell^+\ell^-)$ | $\mathcal{B}(B^- \to \ell^-\bar{\nu})$ | | |
|---|---|---|---|---|---|---|
| | $e^+e^-$ | $\mu^+\mu^-$ | $\mu^+\mu^-$ | $e^-\bar{\nu}$ | $\mu^-\bar{\nu}$ | $\tau^-\bar{\nu}$ |
| SM† | $2 \times 10^{-15}$ | $8 \times 10^{-11}$ | $2 \times 10^{-9}$ | $10^{-15}$ | $10^{-8}$ | $10^{-5}$ |
| UA1 [83] | | $8.3 \times 10^{-6}$ | | | | |
| CLEO [86] | $5.9 \times 10^{-6}$ | $5.9 \times 10^{-6}$ | | $1.5 \times 10^{-5}$ | $2.1 \times 10^{-5}$ | $2.2 \times 10^{-3}$ |
| CDF [89] | | $2.0 \times 10^{-6}$ | $6.8 \times 10^{-6}$ | | | |
| ALEPH [87] | | | | | | $1.8 \times 10^{-3}$ |
| L3 [90] | | | | | | $5.7 \times 10^{-4}$ |

†SM is the Standard Model prediction.[88]

## 1.11 The Search for Mixing and CP Violation in Charm Decays

Predictions of the Standard Model contribution to mixing and CP violation in charm decay are small. Thus, this provides a good place to search for new physics.

The current experimental limit on charm mixing [91] is

$$r_D = \frac{1}{2}\left[\left(\frac{\Delta m_D}{\Gamma}\right)^2 + \left(\frac{\Delta\Gamma}{2\Gamma}\right)^2\right] < 5 \times 10^{-3} \quad , \tag{1.86}$$

while the Standard Model expectation is $\sim 10^{-6}$ [92] [93].

For CP violation the current limit is $\sim$10% [11], while the Standard Model expectation is $\sim 10^{-3}$ [92] [94]. BTeV can probably reach the Standard Model level of CP violation in charm decays. (The $D^{*+}$ provides a wonderful flavor tag.)

# Bibliography


[1] P. Langacker, "CP Violation and Cosmology," in *CP Violation*, ed. C. Jarlskog, World Scientific, Singapore p 552 (1989).

[2] So far CP violation has only been measured in decays of the $K^o$ meson. Results for $\epsilon$ are from 1964. Recent results from KTeV and NA48 are in agreement with earlier measurements from NA31 for a value of $\epsilon'/\epsilon$ on the order of $1 - 22 \times 10^{-4}$. In addition, CDF has seen an indication in $B^o$ decays. T. Affolder *et al*, *Phys. Rev.* **D61** 072005 (2000), hep-ex/9909003.

[3] A. D. Sakharov, *JETP Lett.* **6**, 24 (1967).

[4] N. Cabibbo, *Phys. Rev. Lett.* **10**, 531 (1963); M. Kobayashi and K. Maskawa, *Prog. Theor. Phys.* **49**, 652 (1973).

[5] L. Wolfenstein, *Phys. Rev. Lett.* **51**, 1945 (1983).

[6] S. Stone, "Prospects For B-Physics In The Next Decade," in *Techniques and Concepts of High-Energy Physics IX*, ed. by T. Ferbel, NATO ASI Series, Plenum, NY (1996).

[7] M. Artuso, "Flavour Physics: The Questions, The Clues and the Challenges," Plenary talk at EPS HEP '99, Tampere, Finland, to appear in proceedings, hep-ph/9911347.

[8] R. Aleksan, B. Kayser and D. London, Phys. Rev. Lett. 73 (1994) 18 (hep-ph/9403341).

[9] M. Gaillard and B. Lee, *Phys. Rev.* D10, 897, (1974); J. Hagelin, *Phys. Rev.* D20, 2893, (1979); A. Ali and A. Aydin, *Nucl. Phys.* B148, 165 (1979); T. Brown and S. Pakvasa, *Phys. Rev.* D31, 1661, (1985); S. Pakvasa, *Phys. Rev.* D28, 2915, (1985); I. Bigi and A. Sanda, *Phys. Rev.* D29, 1393, (1984).

[10] J. Rosner, "The Cabibbo-Kobayashi-Maskawa Matrix," in $B$ **Decays,** *Revised 2nd Edition*, ed. S. Stone, World Scientific, Singapore (1994), p470.

[11] Particle Data Group, C. Caso *et al*, The European Physical Journal C3 (1998) 1.

[12] L. Lellouch and C.-J. D. Lin, CERN-TH/99-344 (hep-ph/9912322); D. Becirevic *et al*, ROMA 1285/00 (hep-lat/0002025)

[13] A. J. Buras, "Theoretical Review of B-physics," in *BEAUTY '95* ed. N. Harnew and P. E. Schlein, *Nucl. Instrum. Methods* **A368**, 1 (1995).

[14] S. Stone, "Future of Heavy Flavour Physics: Experimental Perspective," presented at Heavy Flavours 8, June 1999, Southampton, UK to appear in proceedings.

[15] J.L. Rosner, Nucl. Phys. Proc. Suppl. **73** 29, (1999) (hep-ph/9809545).

[16] Private communication from A. Buras.

[17] S. Plaszczynski and M. H. Schune, "Overall Determination of the CKM Matrix," presented at "Heavy Flavours 8," Southampton, UK, July, 1999, to appear in proceedings, hep-ph/9911280.

[18] F. Caravaglios *et al*, "Determination of the CKM Unitarity Triangle Parameters by End of 1999," hep-ph/0002171.

[19] The first papers explaining the physics of mixing and CP violation in $B$ decays were A. Carter and A. I. Sanda, *Phys. Rev. Lett.* 45, 952 (1980); *Phys. Rev.* D23, 1567 (1981); I. I. Bigi and A. I. Sanda, *Nucl. Phys.* B193, 85 (1981); ibid B281, 41 (1987).

[20] I. Bigi, V. Khoze, N. Uraltsev, in **CP Violation**, ed. C. Jarlskog, World Scientific, Singapore 175 (1989).

[21] A. S. Dighe, I. Dunietz, H. J. Lipkin, J. L. Rosner Phys. Lett. B369 144 (1996); R. Fleischer and I. Dunietz, Phys. Lett. B387 361 (1996); Y. Azimov and I. Dunietz Phys. Lett. B395 334 (1997);

[22] M. Beneke, G. Buchalla, I. Dunietz, *Phys. Rev.* D **54**, 4419 (1996).

[23] I. Dunietz, *Phys. Rev.* **D52**, 3048 (1995).

[24] If $\Delta\Gamma$ is non-zero and there is large Penguin amplitude contributing, the lifetime distribution is not a simple exponential. However, using a $\Delta\Gamma$ of 15% and a ratio of Penguin to Tree rates of 4 to 1, we find only a 1% effect on the lifetime.

[25] For the exact formulae see I. Bigi and A. Sanda, "CP Violation," Cambridge (1999), p 183.

[26] A. Dighe, I. Dunietz, and R. Fleischer, *Phys. Lett.* **B433**(1998) 147-149 (hep-ph/9804254).

[27] I. Dunietz, H. Quinn, A. Snyder, W. Toki, and H.J. Lipkin, Phys. Rev. D **43** (1991) 2193.

[28] A.S. Dighe, I. Dunietz, H.J. Lipkin and J.L. Rosner, Phys. Lett. B **369** (1996) 144.

[29] See, for example, M. Jacob and G.C. Wick, Ann. Phys. (N.Y.) **7** (1959) 404.

[30] C. P. Jessop, *et al.* (CLEO). Phys. Rev. Lett. 79, 4533 (1997).

[31] A. Ribon, "B-Physics at the Tevatron Collider," presented at Les Rencontres de Physique de la Valle d'Aoste, La Thuile, Italy, Feb. 28-March 6, 1999.

[32] B. Kayser, "Cascade Mixing and the CP-Violating Angle Beta," in Les Arcs 1997, Electroweak Interactions and Unified Theories, p389 (hep-ph/9709382). Previous work in this area was done by Y. Aimov, Phys. Rev. **D42**, 3705 (1990).

[33] D-S. Du and Z-T. Wei, "Test of CPT Symmetry in Cascade Decays," hep-ph/9904403 (1999).

[34] A. Gritsan "Charmless Hadronic $B$ Meson Decays with CLEO," presented at Lake Louise Winter Institute 2000, to appear in proceedings.

[35] M. Gronau, *Phys. Rev. Lett.* 63, 1451 (1989); M. Gronau and D. London, *Phys. Rev. Lett.* 65, 3381 (1990).

[36] The theoretical accuracy of this approach is limited by electroweak penguins, that are expected to be rather small in this case. In principle, they can be taken into account, as pointed out by Buras and Fleischer in hep-ph/9810260, and also by Gronau, Pirjol and Yan in hep-ph/9810482.

[37] N. G. Deshpande, X. G. He, and S. Oh, Phys. Lett. B384 (1996) 283-287 (hep-ph/9604336), and references therein.

[38] A. E. Snyder and H. R. Quinn, Phys. Rev. D. **48**, 2139 (1993).

[39] Y. Gao and F. Wurthwein, "Charmless Hadronic $B$ Decays at CLEO," in DPF99 proceedings, hep-ex/9904008.

[40] A. Ali, G. Kramer, and C.D. Lu, *Phys. Rev.* **D59** (1999) 014005 (hep-ph/9805403).

[41] H. R. Quinn and J. P. Silva, "The Use of Early Data on $B \to \rho\pi$ Decays," hep-ph/0001290.

[42] A. Deandrea *et al*, "Measuing $B \to \rho\pi$ Decays and the Unitarity Angle Alpha," hep-ph/0002038.

[43] Y. Grossman and H. R. Quinn, "Removing Discrete Ambiguities in CP Asymmetry Measurments," hep-ph/9705356 (1997).

[44] D. Du, I. Dunietz and Dan-di Wu, Phys. Rev D34, 3414 (1986). R. Aleksan, I Dunietz, and B. Kayser, Z. Phys. C54, 653 (1992). R. Aleksan, A. Le Yaouanc, L. Oliver, O. Pène and J.-C. Raynal, Z. Phys. **C67** (1995) 251 (hep-ph/9407406).

[45] D. Atwood, I. Dunietz and A. Soni, *Phys. Rev. Lett.* **78**, 3257 (1997).

[46] M. Gronau and D. Wyler, *Phys. Lett.* B **265**, 172 (1991).

[47] Y. Kwon *et al* (CLEO), "Study of Charmless Hadronic $B$ Decays into the Final States $K\pi$, $\pi\pi$ and $KK$, with the First Observations of $B^o \to \pi^+\pi^-$and $B^o \to K^o\pi^o$," Conf 99-14, hep-ex/9908039 (1999).

[48] R. Fleischer, and T. Mannel, Phys. Rev. D57 (1998) 2752-2759 (hep-ph/9704423).

[49] M. Neubert and J. L. Rosner, Phys. Rev. Lett. 81 (1998) 5076-5079 (hep-ph/9809311).

[50] M. Gronau and J. L. Rosner, Phys. Rev. D57 (1998) 6843-6850 (hep-ph/9711246); M. Gronau, and D. Pirjol, "A Critical Look at Rescattering Effects on $\gamma$ from $B^+ \to K\pi$, hep-ph/9902482 (1999); M. Gronau and J. L. Rosner, "Combining CP Asymmetries in $B \to K\pi$ Decays, hep-ph/9809384 (1998).

[51] J.-M. Gerard and J. Weyers, Eur. Phys. J. **C7** 1(1999) (hep-ph/9711469).

[52] A. Falk, A. Kagan, Y. Nir and A. Petrov, Phys. Rev. **D57** 4290 (1998) (hep-ph/9712225).

[53] M. Neubert, Phys. Lett. **B424** 152 (1998) (hep-ph/9712224).

[54] D. Atwood and A. Soni, Phys. Rev. **D58** 036005 (1998) (hep-ph/9712287).

[55] JHEP 9902:014 (1999) (hep-ph/9812396).

[56] R. Fleischer, Phys. Lett. **B459** 306 (1999) (hep-ph/9903456).

[57] I. Dunietz, "Extracting CKM Parameters from $B$ Decays," in Proceedings of the Workshop on $B$ Physics at Hadron Accelerators, ed. P. McBride and S. Mishra, Snowmass, Co, June (1993), Fermilab-Conf-93/90-T.

[58] For a recent calculation of $\Delta\Gamma_s$, see M. Beneke, G. Buchalla, C. Greub, A. Lenz and U. Nierste, Phys. Lett. **459** 631 (1999) (hep-ph/9808385).

[59] A. Dighe, I. Dunietz, and R. Fleischer, Eur. Phys. J. C6 (1999) 647-662 (hep-ph/9804253).

[60] R. Fleischer and I. Dunietz, Phys. Rev. D55 259 (1997); R. Fleischer, "Extracting CKM Phases from Angular Distributions of $B_{d,s}$ Decays into Admixtures of CP Eigenstates hep-ph/9903540 (1999).

[61] I. Dunietz, Phys. Lett. B427 (1998) 179-182 (hep-ph/97124).

[62] D. Atwood, B. Blok and A. Soni, *Int. J. Mod. Phys.* A11, 3743 (1996); see also N. Deshpande, X. He & J. Trampetic, Preprint OITS-564-REV (1994); see also J. M. Soares, *Phys. Rev.* D53, 241 (1996). G. Eilam, A. Ioannissian R. R. Mendel and P. Singer, *Phys. Rev.* D53, 3629 (1996).

[63] Another method of measuring $|V_{td}|$ is to measure the branching ratio of $K^+ \to \pi^+ \nu\bar{\nu}$. A precise measurement would still be subject to theoretical uncertainties mostly arising from the uncertainty in the charmed quark mass and $|V_{cb}|$ See G. Buchalla, A. J. Buras, and M. E. Lautenbacher, Rev. Mod. Phys., 68, 1125 (1996) (hep-ph/9512380). A Brookhaven experiment, E787, has claimed a signal of one event and hopes to obtain substantially more data. See S. Adler, *et al* (E787), Phys. Rev. Lett 79, 2204 (1997).

[64] Y. Grossman, G. Isidori, M. Worah, Phys. Rev. D58 057504 (1998).

[65] S. J. Richichi *et al* (CLEO) "Two-Body $B$ Meson Decays to $\eta$ and $\eta'$ - Observation of $B \to \eta K^*$" Conf 99-12 (hep-ex/9908019) (1999).

[66] S. Kopp, "Studies of $B^o$ Decays for Measuring $\sin(2\beta)$" presented at DPF'99, to appear in proceedings.

[67] J. P. Silva and L. Wolfenstein, Phys. Rev. **D55** 5331 (1997) (hep-ph/9610208).

[68] Private communication from J. Rosner, A. Buras, C. Bernard and others.

[69] K. Lingel, T. Skwarnicki and J. G. Smith, Ann. Rev. Nucl. Part. Sci. **48** 169 (1998) (hep-ex/9804015).

[70] M. Bander, D. Silverman and A. Soni, *Phys. Rev. Lett.* **43**, 242 (1979).

[71] M. S. Alam *et al* (CLEO), *Phys. Rev. Lett.* **74**, 2885 (1995).

[72] R. Ammar *et al* (CLEO), *Phys. Rev. Lett.* **71**, 674 (1993).

[73] S. Glenn *et al* (CLEO), "Improved Measurement of $\mathcal{B}(b \to s\gamma)$," submitted to XXIX Int. Conf. on High Energy Physics, Vancouver, Canada, July 1998 paper ICHEP98 1011 (1998).

[74] B. Barate *et al* (ALEPH), "A Measurement of the Inclusive $b \to s\gamma$, Branching Ratio," CERN-EP/98-044 (1998).

[75] A. Ali and C. Greub, *Phys. Lett.* B **259**, 182 (1991). The parameters for this fit are $< m_b >$=4.88 GeV and $P_F$ =250 MeV/c.

[76] A. Czarnecki and W. J. Marciano, "Electroweak Radiative Corrections to $b \to s\gamma$," submitted to XXIX Int. Conf. on High Energy Physics, Vancouver, Canada, July 1998 paper ICHEP98 714 (1998); ibid *Phys. Rev. Lett.* **81**, 277 (1998); see also see also M. Neubert, "Theoretical Status of $b \to X_s\gamma$ Decays," hep-ph/9809377 (1998); A. Ali, "Theory of Rare $B$ Decays," hep-ph/9709507 DESY 97-192 (1997); N. G. Deshpande, "Theory of Penguins in $B$ Decays," in *B Decays Revised 2nd Edition*, ed. by S. Stone, World Scientific, Singapore, (1994).

[77] J. L. Hewett, "$B$ Physics Beyond the Standard Model," hep-ph/9803370 (1998).

[78] S. Abachi *et al* (D0), *Phys. Rev.* D **56**, 6742 (1997); F. Abe *et al* (CDF), *Phys. Rev. Lett.* **78**, 4536 (1997).

[79] R. Ammar *et al*, "Radiative Penguin Decays of the B Meson," CLEO-CONF 96-6 (1996).

[80] D. Atwood, B. Blok & A. Soni, *Int. J. Mod. Phys.* **A11**, 3743 (1994) and *Nuovo Cimento* **109A**, 873 (1994); N. Deshpande, X. He & J. Trampetic, *Phys. Lett.* B **362**, 1996 (;) see also J. M. Soares, *Phys. Rev.* D **53**, 241 (1996); G. Eilam, A. Ioannissian & R. R. Mendel, *Z. Phys.* **C71**, 95 (1995).

[81] S. Fukae, C.S. Kim , T. Morozumi, and T. Yoshikawa, "A Model Independent Analysis of the Rare $B$ Decay $B \to X_s \ell^+ \ell^-$, KEK-TH578, hep-ph/9807254 (1998), and references cited therein.

[82] A. Ali, C. Greub and T. Mannel, "Rare B Decays in the Standard Model, " in Hamburg 1992, Proceedings, ECFA Workshop on a European B-meson Factory, Eds. R. Aleksan and A. Ali, p155 (1993).

[83] C. Albajar *et al*, *Phys. Lett.* B262, 163 (1991).

[84] R. Godang *et al*, "Search for Electroweak Penguin Decays $B \to K \ell^+ \ell^-$ and $B \to K^* \ell^+ \ell^-$ at CLEO," CLEO-CONF 98-22 (1998).

[85] T. Affolder *et al* (CDF), Phys. Rev. Lett. 83, 3378 (1999).

[86] R. Ammar *et al*, *Phys. Rev.* D49, 5701 (1994); M. Artuso, *et al*, *Phys. Rev. Lett.* 75, 785 (1995).

[87] D. Buskulic *et al*, *Phys. Lett.* B343, 444 (1995).

[88] A. Ali and T. Mannel, *Phys. Lett.* B264, 447 (1991). Erratum, ibid, B274, 526 (1992).

[89] F. Abe *et al* (CDF), Phys. Rev. D 57, R3811 (1998).

[90] M. Acciarri *et al.* (L3), Phys. Lett. B 396 (1997) 327-337.

[91] E. M. Aitala *et al*, *Phys. Rev. Lett.* **77**, 2384 (1996).

[92] G. Burdman, "Potential for Discoveries in Charm Meson Physics," hep-ph/9508349.

[93] H. Georgi, *Phys. Lett.* **B297**, 353 (1992); T. Ohl *et al*, *Nucl. Phys. B* **403**, 603 (1993).

[94] I. I. Bigi and H. Yamamoto, *Phys. Lett. B* **349**, 363 (1995).